



Archived at the Flinders Academic Commons:

<http://dspace.flinders.edu.au/dspace/>

'This is the peer reviewed version of the following article:

Hosseini, S. M., Ataie-Ashtiani, B., & Simmons, C. T.

(2018). Density-based global sensitivity analysis of sheet-flow travel time: Kinematic wave-based formulations.

Journal of Hydrology, 559, 556–568. <https://doi.org/10.1016/j.jhydrol.2018.02.052>

which has been published in final form at

<http://dx.doi.org/10.1016/j.jhydrol.2018.02.052>

© 2017 Elsevier. This manuscript version is made available under the CC-BY-NC-ND 4.0 license:

<http://creativecommons.org/licenses/by-nc-nd/4.0/>

# Accepted Manuscript

Research papers

Density-based Global Sensitivity Analysis of Sheet-Flow Travel Time: Kinematic Wave-Based Formulations

Seiyed Mossa Hosseini, Behzad Ataie-Ashtiani, Craig T. Simmons

PII: S0022-1694(18)30129-X

DOI: <https://doi.org/10.1016/j.jhydrol.2018.02.052>

Reference: HYDROL 22601

To appear in: *Journal of Hydrology*

Received Date: 24 January 2018

Revised Date: 14 February 2018

Accepted Date: 16 February 2018

Please cite this article as: Hosseini, S.M., Ataie-Ashtiani, B., Simmons, C.T., Density-based Global Sensitivity Analysis of Sheet-Flow Travel Time: Kinematic Wave-Based Formulations, *Journal of Hydrology* (2018), doi: <https://doi.org/10.1016/j.jhydrol.2018.02.052>

This is a PDF file of an unedited manuscript that has been accepted for publication. As a service to our customers we are providing this early version of the manuscript. The manuscript will undergo copyediting, typesetting, and review of the resulting proof before it is published in its final form. Please note that during the production process errors may be discovered which could affect the content, and all legal disclaimers that apply to the journal pertain.



# Density-based Global Sensitivity Analysis of Sheet-Flow Travel Time: Kinematic Wave-Based Formulations

Seiyed Mossa Hosseini<sup>a,1</sup>, Behzad Ataie-Ashtiani<sup>b,c</sup>, Craig T. Simmons<sup>c</sup>

<sup>a</sup>Physical Geography Department, University of Tehran, P.O. Box 14155-6465, Tehran, Iran.

<sup>b</sup>Department of Civil Engineering, Sharif University of Technology, P.O. Box 11155-9313, Tehran, Iran

<sup>c</sup>National Centre for Groundwater Research & Training and College of Science & Engineering, Flinders University, GPO  
Box 2100, Adelaide, South Australia 5001, Australia.

## Abstract

Despite advancements in developing physics-based formulations to estimate the sheet-flow travel time ( $t_{SHF}$ ), the quantification of the relative impacts of influential parameters on  $t_{SHF}$  has not previously been considered. In this study, a brief review of the physics-based formulations to estimate  $t_{SHF}$  including kinematic wave (K-W) theory in combination with Manning's roughness (K-M) and with Darcy-Weisbach friction formula (K-D) over single and multiple planes is provided. Then, the relative significance of input parameters to the developed approaches is quantified by a density-based global sensitivity analysis (GSA). The performance of K-M considering zero-upstream and uniform flow depth (so-called K-M1 and K-M2), and K-D formulae to estimate the  $t_{SHF}$  over single plane surface were assessed using several sets of experimental data collected from the previous studies. The compatibility of the developed models to estimate  $t_{SHF}$  over multiple planes considering temporal rainfall distributions of Natural Resources Conservation Service, NRCS (I, Ia, II, and III) are scrutinized by several real-world examples. The results obtained demonstrated that the main controlling parameters of  $t_{SHF}$  through K-D and K-M formulae are the length of surface plane (mean sensitivity index  $\hat{T}_i=0.72$ ) and flow resistance (mean  $\hat{T}_i=0.52$ ), respectively. Conversely, the flow temperature and initial abstraction ratio of rainfall have the lowest influence on  $t_{SHF}$ .

---

<sup>1</sup> Corresponding Author. *Email address:* [smhosseini@ut.ac.ir](mailto:smhosseini@ut.ac.ir) (S.M. Hosseini).

28 (mean  $\hat{T}_i$  is 0.11 and 0.12, respectively). The significant role of the flow regime on the  
29 estimation of  $t_{SHF}$  over a single and a cascade of planes are also demonstrated. Results  
30 reveal that the K-D formulation provides more precise  $t_{SHF}$  over the single plane surface  
31 with an average percentage of error, APE equal to 9.23% (the APE for K-M1 and K-M2  
32 formulae were 13.8%, and 36.33%, respectively). The superiority of Manning-jointed  
33 formulae in estimation of  $t_{SHF}$  is due to the incorporation of effects from different flow  
34 regimes as flow moves downgradient that is affected by one or more factors including  
35 high excess rainfall intensities, low flow resistance, high degrees of imperviousness, long  
36 surfaces, steep slope, and domination of rainfall distribution as NRCS Type I, II, or III.

37  
38 **Key-Words:** Unit hydrograph, Sheet-flow, Travel time, Kinematic wave, Sensitivity Analysis,  
39 Flow regime.

40

## 41 1. Introduction

42 Sheet-flow travel time ( $t_{SHF}$ ) is defined as the time that excess-rainfall originated from  
43 rainfall, snowmelt, and saturation excess on the soil surface moves from the furthest  
44 segment of the drainage path which is located immediately downstream from the  
45 drainage divide line to the nearest stream or becomes shallow-concentrated flow (NRCS,  
46 1986; Yamoto and Islam 1992). This compartment contributes an important part of the  
47 time of concentration of watershed to develop the unit hydrograph (Froelich, 2011) and  
48 selecting the design storm intensity for estimation of watershed peak-outflow (Bondelid  
49 et al., 1982). Almost all hydrologic analyses and modelling require the value of time  
50 response characteristics as input (McCuen et al., 1984; Paniconi and Putti, 2015).

51 Compared with the other compartments of time of concentration of watershed (i.e.  
52 shallow-concentrated and stream-flow),  $t_{SHF}$  is likely to be the dominant component for  
53 small watersheds, parking lots, rooftops, highways, airport runways, artificially

54 constructed wetlands, agricultural plots, and lawns (Singh, 2002) and at the same time, is  
55 the most theoretically questionable of the three compartments (Dewberry, 2003). These  
56 challenges arise mainly from non-homogeneity in land cover and land use as major  
57 characteristics of micro and partly urbanized watersheds that certainly affect the sheet-  
58 flow properties (i.e. travel time and flow depth). Developed formulations to estimate  $t_{SHF}$   
59 are an important step to partially compensate for this challenge.

60 Since Lighthill and Whitham (1955) and thereafter Miller and Gunge (1975) showed that  
61 inertial and pressure forces are not important for overland flow during storm events due  
62 to the domination of the bed slope term in the motion equation, an increasing number of  
63 applications of the kinematic wave (K-W) theory are reported for developing physics-  
64 based formulations for accurate and efficient estimation of  $t_{SHF}$  over single (Overton and  
65 Meadows, 1976; SCS, 1986; Wong and Chen, 1997) or multiple continuous planes (e.g.  
66 Kibler and Woolhiser, 1972; Wong 1996).

67 Whereas successive progressions were obtained by combining the K-W theory with the  
68 Manning's resistance formulation (K-M) to estimate  $t_{SHF}$  over a single plane (NRCS,  
69 1986; ASCE, 1992; Overton and Meadows, 1976; Froehlich, 2011); two planes in V-  
70 shape geometry (Overton and Eagleson, 1970; Singh, 1996); multiple plane surfaces  
71 (Brakensiek, 1967; McCuen and Okunola, 2002); converged hillslope (Veal, 1966),  
72 diverged hillslope (Campbell and Parlange, 1984) and complex-shaped hillslope  
73 (Sabzevari et al. 2013); and watershed geometry and leaf-shape water geometry  
74 (Agiralioglu, 1985). However, this formulation was limited to turbulent or near turbulent  
75 sheet-flow regime over the whole surface plane. Further simplifications accompanied by  
76 the K-W approach are ignoring the effects of momentum due to sheet-flow and rain  
77 (Langford and Turner, 1973), and considering one-dimensional sheet-flow and uniform  
78 distribution of rainfall over the plane surface.

79 As sheet-flow is characterized by a small hydraulic radius (i.e. flow depth) and slow  
80 velocity at the upgradient region, the flow regime should not be considered fully  
81 turbulent over the surface plane (Bulter, 1977). Combining K-W theory with the Darcy-  
82 Weisbach friction formulation (K-D) incorporates the effect of different flow regime  
83 (laminar, transitional, and turbulent) to estimate  $t_{SHF}$  (Singh 1988; Wong and Chen,  
84 1997). Field and laboratory studies on  $t_{SHF}$  seem to use the K-D equation whilst the K-M  
85 equation is frequently used for channel flow (Abraham et al., 1990). However, selecting  
86 the type of equation for estimation of  $t_{SHF}$  appears to be much more influenced by  
87 personal preference rather than the real properties of sheet-flow. Probably one of the  
88 reasons that hydrologists tend to use K-M rather than K-D is the lack of data sources for  
89 Manning's roughness coefficient ( $n$ ) compared with the Darcy-Weisbach coefficient ( $f$ ),  
90 and also the uncertainties in  $f$  values for different flow regimes and surfaces (Grismer,  
91 2016).

92 The input parameters for these formulations can be categorized as 1) physical properties  
93 of the plane surface including soil type, land use, land cover, surface slope, flow  
94 resistance (roughness), and length of surface in direction of flow; and 2) storm and  
95 weather conditions including the temporal and spatial distribution of rainfall intensity,  
96 average daily rainfall, temperature, and initial abstractions related to climate conditions.  
97 However, previous works report that the parameters which have the dominant influence  
98 upon  $t_{SHF}$  in the catchment are length, slope, roughness and flow regime (e.g. Wooding,  
99 1965). No attempt has been made to systematically and quantitatively indicate the relative  
100 impact of these influential parameters on the  $t_{SHF}$ . In addition, applications of developed  
101 models have been mainly limited to hypothetical examples that did not fully match with  
102 real-world conditions. To fill these gaps, the main objective of this study is to obtain the

103 relative influence of input parameters of kinematic wave-based formulations to estimate  
104  $t_{SHF}$  by a density-based global sensitivity analysis (GSA) for the first time.

105 An integrated assessment of the developed formulations to estimate the  $t_{SHF}$  and the  
106 degree of conformity of their results with experimental data and also practical conditions  
107 are scrutinized for the first time by considering a single plane. The overall flowchart of  
108 the research methodology is shown in Fig. 1. The performance of the developed formulae  
109 to estimate the  $t_{SHF}$  are also assessed through multiple continuous planes by using  
110 numerous real-world systems of hillslope-riparian-stream hydrologic connectivity where  
111 the temporal variation of rainfall intensity is also considered. A brief review of the K-W  
112 based formulations on the estimation of  $t_{SHF}$  is given in the next section.

113

## 114 **2. Research Background for $t_{SHF}$ over Single and Multiple Planar Surfaces**

115 The kinematic wave (K-W) model, in addition to the diffusion, full- and steady dynamic,  
116 and gravity wave models, is a distinctive approximation of the Saint-Venant equation  
117 (Ponce and Simons, 1977). According to Table 1, the K-W model is based on the  
118 continuity equation and only approximates the dynamic equation so that the friction slope  
119 is parallel to the bed slope (Miller, 1983). The K-W gives a valid approximation for  
120 hydraulics of one dimensional, shallow, unsteady and uniform flow travelling down  
121 across planar (or wide) surfaces in the absence of backwater effects and incompressibility  
122 of flow, as shown in Fig. 2 (Lighthill and Witham, 1955; Wooding 1965; Singh, 1996):

$$\frac{\partial y}{\partial t} + \frac{\partial q}{\partial x} = i - I \quad (1)$$

123 where  $y$  is depth of flow perpendicular to plane surface [ $L$ ],  $q$  is unit discharge [ $L^2 T^{-1}$ ],

124  $i$

125 is average rate of distributed inflow per unit area due to rainfall [ $L T^{-1}$ ],  $I$  is losses due to

126 interception, infiltration, and surface storage [ $L T^{-1}$ ],  $t$  is the time since excess rainfall

127 appears  $[T]$ , and  $x$  is distance along the plane in flow direction  $[L]$ . The right hand side of  
 128 Eq. 1 can be replaced by the average excess rainfall intensity  $i_e$  (e.g. Singh 2001, García-  
 129 Serrana et al., 2017). The K-W model uses the continuity and simplified form of the motion  
 130 equation such that the friction slope is equal to the bed slope and, therefore, does not change  
 131 with flow conditions. The K-W approximation, which also denotes the quasi-steady  
 132 condition (Wooding, 1965), is also valid when the Froude number of sheet-flow is less  
 133 than or equal to two,  $Fr \leq 2$  (Miller, 1983). The equation of motion states that the lateral  
 134 inflow ( $q$ ) is related to flow depth ( $y$ ) only by using two coefficients  $\alpha$  and  $\beta$  in Eq. 2  
 135 under the assumption that the hydraulic radius of sheet-flow,  $R_h [L]$  equal to  $y$  (Eagleson,  
 136 1970; Singh, 2001):

137

$$q = \alpha y^\beta \quad (2)$$

138 Where  $\alpha [-]$  is a resistance parameter and reflects the interaction between the fluid  
 139 particles themselves and between the fluid and the surface boundary and whose value  
 140 varies in space and time. The parameter  $\beta [-]$  is an exponent indicating the regime of  
 141 flow and degree of nonlinearity which varies from 1 (highly turbulent) to 3 (laminar)  
 142 (Singh, 2002). Two coefficients  $\alpha$  and  $\beta$  can be defined by the Darcy-Weisbach friction  
 143 formula using Eq. 3 (for laminar, transitional, and turbulent flow regimes) or by the  
 144 Manning's resistance formula using Eq. 4 (for turbulent or near turbulent flow regime)  
 145 regardless of their spatial and temporal heterogeneities (Julien and Simons, 1985):

146

$$\left\{ \begin{array}{ll} \alpha = \frac{8 g S}{\tau_1 v} ; \quad \beta = 3 & \text{for laminar flow} \quad (3 - a) \\ \alpha = \left( \frac{8 g S}{\tau_2 v^k} \right)^{\frac{1}{2-k}} ; \quad \beta = \frac{3}{2-k} ; \quad 0 < k < 1 & \text{for transitional flow} \quad (3 - b) \\ \alpha = \left( \frac{8 g S}{\tau_3} \right)^{1/2} ; \quad \beta = \frac{3}{2} & \text{for turbulent flow} \quad (3 - c) \end{array} \right.$$



$$\alpha = \frac{\sqrt{S}}{n} ; \quad \beta = \frac{5}{3} \quad (4)$$

147 where  $g$  is gravity acceleration [ $L T^{-2}$ ],  $S$  is slope of surface plane in flow direction  
 148 [ $L L^{-1}$ ],  $\nu$  is kinematic viscosity of sheet-flow [ $L^2 T^{-1}$ ],  $\tau$  is a constant value that related  
 149 Reynolds number ( $R_e$ ) to the Darcy-Weisbach resistance coefficient ( $f$ ) through the  
 150  $f = \tau_1/R_e$  (for laminar flow),  $f = \tau_2/R_e^k$ ,  $0 < k < 1$  (for transitional flow), and  $f = \tau_3$   
 151 (for turbulent flow) (Wenzel, 1970). Solving the first-order hyperbolic differential  
 152 equation of Eq. 1 by the method of characteristics yields a nearly analytic solution for  
 153 celerity of the wave,  $\omega$  [ $L T^{-1}$ ] that, therefore, involves very little numerical dispersion  
 154 (Crandall, 1956):

$$\omega = \frac{dx}{dt} = \frac{dq}{dy} ; \quad \frac{dy}{dt} = i_e \quad (5)$$

155 Integrating Eq. 5 with respect to  $x = 0 \rightarrow L$ ,  $t = 0 \rightarrow t_t$ , and considering the upstream  
 156 boundary condition (i.e.,  $q_{x=0} = q_u$ , where  $u$  denotes upstream), the travel time for a  
 157 planar surface,  $t_{SHF}$  can be obtained (Wong, 1996; Beldring *et al.*, 2000):

158

$$t_{SHF} = \frac{q_d^{1/\beta} - q_u^{1/\beta}}{\alpha^{1/\beta} i_e} ; \quad q_d = q_u + i_e L \quad (6)$$

159 where  $L$  is the total length of plane in flow direction [ $L$ ]. According to K-W theory, Eq. 1  
 160 defines the travel time as the time needed for establishing the equilibrium state for  
 161 discharge (i.e. inflow =outflow) at any point of interest over the surface plane (ASCE,  
 162 1992; Akan, 1986).

163 For zero up-stream boundary condition (i.e.  $q_u=0$ ), and considering turbulent flow over  
 164 the entire surface (replacing  $\alpha$  and  $\beta$  by Manning formula, Eq. 4), Eq. 6 reduces to that  
 165 obtained by the previous studies (i.e. Wong, 1994; Henderson and Wooding, 1964):

166

$$t_t = \left(\frac{L}{\alpha}\right)^{1/\beta} i_e^{\frac{1}{\beta}-1} \rightarrow t_t = \frac{\gamma}{i_e^{0.4}} \left(\frac{Ln}{S^{0.5}}\right)^{0.6} \quad (7)$$

167 where  $\gamma$  is conversion factor of units.  $\gamma = 9.80$  for SI units (min for  $t_t$ , m for  $L$ ,  $\text{m} \cdot \text{m}^{-1}$  for  
 168  $S$ , and  $\text{mm} \cdot \text{hr}^{-1}$  for  $i_e$ ), and  $\gamma = 1.315$  for the British Imperial (BG) units (min for  $t_t$ , ft for  
 169  $L$ ,  $\text{ft} \cdot \text{ft}^{-1}$  for  $S$ , and  $\text{in} \cdot \text{hr}^{-1}$  for  $i_e$ ), and  $n [L^{-1/3} T]$  is Manning's roughness coefficient.  
 170 Some studies (i.e. Ragan and Duru, 1972; Overton and Meadow, 1976) obtained  $t_t$   
 171 equation by considering uniform flow depth over the planar surface ( $y_{x=0 \rightarrow L} = y$ ) with  
 172 keeping turbulent flow assumption. A schematic watershed and the above mentioned  
 173 variables are shown in Fig. 2. Assuming uniform flow depth over the surface reduces the  
 174 conversion factor  $\gamma$  to 6.988, and 1.40 for SI and BG units, respectively. However,  
 175 employing a zero-upstream boundary condition to obtain the  $t_t$  (Eq. 7) gives a greater  
 176 travelling time by a factor of 1.4, but it is more realistic and coincides with real cases as  
 177 flow depth (or flow velocity,  $V [L T^{-1}]$ ) increases as flow travels to the downstream of  
 178 the surface, such that the maximum depth (or  $V$ ) occur at downstream edge of surface  
 179 ( $y_{x=L} = y_{max}$ ,  $V_{x=L} = V_{max}$ ). Applying uniform flow depth over the surface assumed  
 180 identical flow velocity over the planar surface which is equal to  $V_{max}$ . It should be noted  
 181 that Eqs. (6 and 7) are valid if the parameters of  $S$ ,  $n$ ,  $i_e$  (i.e. infiltration), and flow regime  
 182 (i.e. turbulent) are constants over the plane surface (Wong, 1996). Considering the zero-  
 183 upstream flow condition, and therefore flow-depth growth, implies a changing flow  
 184 regime from laminar, at the upstream edge through transitional, at the middle distance to  
 185 turbulent flow, at the downstream edge. If the Reynolds number is defined as  $Re =$   
 186  $V \cdot R_h / \nu = q_d / \nu$  (Savat, 1977), the critical values of  $Re$  for changing the flow regimes  
 187 yields the portion of plane length with laminar ( $L_1$ ), transitional ( $L_2$ ), and turbulent ( $L_3$ )  
 188 flow regime as follows (Wong and Chen, 1997):

$$L_1 = \frac{\delta \nu Re_1}{i_e} ; L_2 = \frac{\delta \nu (Re_2 - Re_1)}{i_e} ; L_3 = L - (L_1 + L_2) ; \delta = 3.6 \times 10^6 \quad (8)$$

189 where  $Re_1$ , and  $Re_2$  are critical Reynolds numbers for the laminar, and the transitional  
 190 flow regime over the plane, respectively. According to Wenzel (1970),  $Re_1$  and  $Re_2$  are  
 191 assumed equal to 200 and 2000, respectively. As the plane surface is continuous, the unit  
 192 discharge ( $q$ ) changes between  $[q_u = 0, q_d = i_e L_1/\delta]$ ,  $[q_u = i_e L_1/\delta, q_d = i_e (L_1 +$   
 193  $L_2)/\delta]$ , and  $[q_u = i_e (L_1 + L_2)/\delta, q_d = i_e L/\delta]$  for the portion of plane with laminar,  
 194 transitional, and turbulent regime, respectively. Considering these boundary conditions,  
 195 and also the length of flow with different regimes (Eq. 8), the final form of  $t_{SHF}$  based on  
 196 the kinematic wave solution for single planar surface in conditions of constant  $S$ ,  $n$ ,  $i_e$ ,  
 197 water temperature, and absence of back water is as  $t_{SHF} = t_1 + t_2 + t_3$ , where  $t_1$ ,  $t_2$ , and  
 198  $t_3$  are sheet-flow travel time for laminar, transitional, and turbulent flow portion, defined  
 199 respectively as (Wong and Chen, 1993)

$$t_1 = 0.595 \left( \frac{\delta \nu f Re_1 L_1}{S i_e^2} \right)^{1/3} \quad \text{for } 0 \leq x \leq L_1 \text{ or } Re < Re_1 \quad (9)$$

$$t_2 = 0.595 \left( \frac{f (Re_2 \delta \nu)^k}{S i_e^{k+1}} \right)^{1/3} \times \left[ (L_1 + L_2)^{\frac{2-k}{3}} - L_1^{\frac{2-k}{3}} \right]$$

$$\text{for } L_1 \leq x \leq L_2 \text{ or } Re_1 < Re < Re_2 \quad (10)$$

$$t_3 = 0.595 \times \left( \frac{f}{S i_e} \right)^{1/3} \times \left[ L^{2/3} - (L_1 + L_2)^{2/3} \right] \quad \text{for } L_2 \leq x \leq L \text{ or } Re > Re_2 \quad (11)$$

200 For laminar and transitional sheet-flow regimes on a given surface (i.e.  $Re < 2000$ ), the  
 201 flow resistance ( $f$ ) increases by the growth of the flow depth (or excess rainfall  
 202 intensity), whereas for the higher Reynolds number, the effect of intensity becomes  
 203 insignificant (Zoltani, 1992). The relations of  $f$  and  $Re$  for laminar, transitional, and  
 204 turbulent flows are  $f = \tau_1/Re$ ,  $f = \tau_2/\sqrt{Re}$ , and  $f = \tau_3$ , respectively. Constants of  $\tau_1$ ,  
 205  $\tau_2$ , and  $\tau_3$  are a function of surface slope and rainfall intensity (or flow depth) which can

206 be obtained from the previous analysis on different surfaces (i.e. Phelps, 1970; Wenzel,  
207 1970; Radojkovic and Maksimovic, 1986).

208 Estimation of  $t_{SHF}$  using the Manning formula is valid for turbulent or near turbulent  
209 flow regimes in two conditions of zero-upstream ( $y_u = 0$ ) and uniform flow depth over  
210 the planar surface ( $y_u = y_d$ ) (McCuen and Okunola, 2002):

$$t_{SHF} = \begin{cases} 6.988 \times \left( \frac{n L}{\sqrt{S} i_e^{2/3}} \right)^{3/5} & \text{for } y_u = 0 & (12 - a) \\ 4.984 \times \left( \frac{n L}{\sqrt{S} i_e^{2/3}} \right)^{3/5} & \text{for } y_u = y_d & (12 - b) \end{cases}$$

211 The current version of Natural Resources Conservation Service (NRCS) software, TR-55  
212 (SCS, 1986), regardless of flow regime, considers a maximum length of 300 feet (~100  
213 m) for sheet-flow or the distance between the drainage divide and the upper end of a  
214 defined stream (each one is smaller). After this distance, even if the plane surface  
215 continues, the sheet-flow becomes shallow-concentrated flow.

216

### 217 2.1. Goodness of K-W Theory to Estimate $t_{SHF}$

218 Despite numerous studies successfully applying the K-W theory for modelling overland  
219 flow, Woolhiser and Liggett (1967) derived a criterion referred to as the kinematic wave  
220 number ( $\eta$ ) for judging the goodness of the K-W approximation in modelling of sheet-  
221 flow over a sloping plane

$$\eta = \frac{S L}{y Fr^2} \quad (13)$$

222 All variables in Eq. 13 are defined previously. Substituting  $Fr = V/\sqrt{g y}$ , Eq. 13  
223 reduces to

$$\eta = \frac{S g L}{V^2} \quad (14)$$

224 Woolhiser and Liggett (1967) indicated that for  $\eta > 50$ , the K-W approximation would be  
 225 very good. Replacing  $g=9.81 \text{ m s}^{-2}$  in Eq. 14,  $S L/V^2$  should be greater than 2.04 to  
 226 have good approximation with K-W theory (units of  $V$  and  $L$  are  $\text{m s}^{-1}$  and  $\text{m}$ ,  
 227 respectively) which is valid for sheet-flow over numerous natural surfaces. Therefore, the  
 228 criterion of  $\eta$  needs to check only for smooth surfaces in which applying the K-W theory  
 229 may produce a crude approximation (for example, in urban surfaces  $\eta$  may be below 20).  
 230 Another goodness of fit criteria was suggested by McCuen and Spiess (1995) which  
 231 implies that the K-W assumption should be limited to the kinematic wave number  
 232  $N_{K-W} = nl/\sqrt{S} < 100$ .

233

### 234 2.2. Estimation of excess rainfall intensity, $i_e$

235 In Eqs. (9) to (12),  $i_e$  is the average excess rainfall intensity for the storm with duration  
 236 equal to  $t_t$  ( $D = t_t$ ), therefore repeated solution of these equations are required to find an  
 237 appropriate value of  $D$  that is equal to  $t_t$ . To eliminate this repetition problem, Chen and  
 238 Evan (1977) proposed the use of an intensity-duration relation ( $i - D$ ) in the form of  
 239  $i = a \times D^{-b}$  (where  $a$  and  $b$  are regional constants) in the Manning formula (Eq. 12).  
 240 Average rainfall intensity ( $i$ ) is related to  $i_e$  by a runoff coefficient ( $C$ ) through the  
 241 rational formula of  $i_e = C \times i$  (ASCE, 1992). Welle and Woodward (1986) used  $i - D$   
 242 relations for two NRCS standard design storms Type II and III in the form of  $i =$   
 243  $a' \times P_{24} \times D^{-b'}$ , where  $P_{24}$  is 24-hr rainfall depth in mm, and constants  $a'$  and  $b'$  are 5.7  
 244 and -0.62 (for storm Type II), and 4.76 and -0.63 (for storm Type III), respectively. The  
 245 NRCS design storms I, Ia, II, and III are characterized by an intense rainfall period  
 246 somewhere near the middle and lesser rainfall intensities at the beginning and end of the  
 247 storm and have been applied to very large geographic regions (Cronshey and Woodward,  
 248 1989). For instance, the Type II distribution has been applied to a large part of the central

249 continental United States, and Type Ia has been used in the Pacific Northwest (SCS,  
250 1973).

251 TR-55 model uses a modified form of the Manning formula (Eq. 12) in which  $i_e$  is  
252 replaced by 2-years  $P_{24}$ :

$$t_{SHF} = \frac{5.5}{\sqrt{P_{24}}} \times \left( \frac{nL}{\sqrt{S}} \right)^{4/5} \quad (15)$$

253 However, using  $i - D$  relations in the estimation of  $t_{SHF}$  solves the repetition problem,  
254 but leads to different results as reported by McCuen and Spiess (1995). Froehlich (2009)  
255 showed that estimation of  $t_{SHF}$  with the Manning formula and  $i - D$  relations proposed  
256 by Welle and Woodward (1986) produces significant error especially for a small  
257 duration, i.e.  $D < 15$  min. Precise estimation of  $i$  for four types of rainfall distributions of  
258 NRCS and wide range of  $D$  were proposed by Froehlich (2009) as

$$i_e = C \times \begin{cases} 16.138 \times \frac{P_{24}}{D} \times (1 - e^{-0.049 \times D}) + 0.0305 \times P_{24} & \text{for storm Type I} \\ 13.963 \times \frac{P_{24}}{D} \times (1 - e^{-0.017 \times D}) + 0.0322 \times P_{24} & \text{for storm Type Ia} \\ 26.911 \times \frac{P_{24}}{D} \times (1 - e^{-0.0601 \times D}) + 0.0231 \times P_{24} & \text{for storm Type II} \\ 26.998 \times \frac{P_{24}}{D} \times (1 - e^{-0.033 \times D}) + 0.0230 \times P_{24} & \text{for storm Type III} \end{cases} \quad (16)$$

259 Alternate formulation of Eq. (16), which is also used in this study, is the estimation of  
260 runoff coefficient ( $C$ ) through Soil Conservation Service Curve Number (SCS-CN)  
261 method (Hawkins, 1983):

$$C = \frac{R}{P} = \frac{1}{P} \times \left[ \frac{\left( P - \lambda \times \left( \frac{25400}{CN} - 254 \right) \right)^2}{P + (1 - \lambda) \times \left( \frac{25400}{CN} - 254 \right)} \right] \quad (17)$$

262 where  $R$  is direct runoff depth in  $mm$ ,  $P$  is rainfall depth in  $mm$ ,  $\lambda$  is initial abstraction  
263 ratio, and  $CN$  is the curve number. Combining Eq. (16) and (17) one can estimate the  
264 average excess rainfall intensity ( $i_e$ ) for different temporal rainfall distributions of NRCS.

265

## 266 2.3. Multiple Planar Surfaces

267 In the previous section, the approaches for estimation of  $t_{SHF}$  over a plane surface are  
 268 presented, in which the input parameters (e.g. slope and roughness) are homogeneous  
 269 over the surface. This condition is more consistent with sheet-flow that occurs in the  
 270 furthest upstream segment of the drainage path or across the street in an urban area.  
 271 Commonly, sheet-flow from a wooded area may flow onto a dense grass-covered surface,  
 272 which may then discharge onto a paved surface, such as a driveway, and continue over  
 273 the rangeland or turf (as shown in Fig. 3). Each of these surfaces has a different resistance  
 274 to flow or roughness and hydraulic radius and may differ in slope and infiltration. Thus,  
 275 equations that assume a single section that is homogeneous in land cover, hydraulic  
 276 radius, and roughness (i.e. one used in TR-55), cannot be applied (McCuen and Okunola,  
 277 2002).

278 The assumptions of zero-upstream boundary conditions ( $q_u = 0$ ) and uniform flow  
 279 distribution ( $q_u = q_d$ ) behind Eq. (12) that lead to these formulae cannot be applied  
 280 precisely for the cascade of surface planes. For a multi-planar flow path with  $N$  planes in  
 281 which flow from an upgradient plane discharges onto the next down-gradient plane, Eqs.  
 282 (9-12 and 15-17) should be extended. Wong (1996) derived the kinematic wave and  
 283 Manning formula for estimation of  $t_{SHF}$  for a series of planes. The general form of  $t_{SHF}$   
 284 formulation for cascade of  $N$  planes is as follows:

$$t_{SHF} = \sum_{j=1}^N \frac{L_j}{\alpha_j^{1/\beta_j}} \left\{ \frac{[\sum_{m=1}^j (i_{e_m} L_m)]^{1/\beta_j} - [\sum_{m=1}^{j-1} (i_{e_m} L_m)]^{1/\beta_j}}{[\sum_{m=1}^j (i_{e_m} L_m)] - [\sum_{m=1}^{j-1} (i_{e_m} L_m)]} \right\} \quad (18)$$

285 where  $j$  is index for planes in direction of sheet-flow. Eq. (18) is based on the  
 286 assumption that downstream outflow of one plane becomes the inflow to the adjacent  
 287 plane downstream, without backwater condition, and all surfaces contribute in runoff

288 generation. Replacing the values of  $\alpha$  and  $\beta$  from Eqs. 3(a-c) corresponding to the flow  
 289 regime in each section, reduces Eq. (18) to a kinematic wave approximation. The  
 290 Manning expression for estimation of the  $t_{SHF}$  over continuous multi-planar surface for  
 291 turbulent or near turbulent flow regimes (so called K-M3) can be obtained with  
 292 parameters  $\alpha$  and  $\beta$  from Eq. (4) employed in Eq. 18 as follows:

$$t_{SHF} = \sum_{j=1}^N 6.988 L_j \left( \frac{n_j}{\sqrt{S_j}} \right)^{0.6} \left\{ \frac{[\sum_{m=1}^j (i_{e_m} L_m)]^{0.6} - [\sum_{m=1}^{j-1} (i_{e_m} L_m)]^{0.6}}{[\sum_{m=1}^j (i_{e_m} L_m)] - [\sum_{m=1}^{j-1} (i_{e_m} L_m)]} \right\} \quad (19)$$

293

### 294 3. Global Sensitivity Analysis

295 Global Sensitivity Analysis (GSA) is a useful tool in understanding the relative  
 296 influences of the different sources of uncertainty (e.g. model parameters, errors in forcing  
 297 data, or non-numerical uncertainties) in the variability of the model output (Saltelli *et al.*;  
 298 2008, Baroni and Tarantola, 2014; Rajabi *et al.*, 2015). Density-based sensitivity indices  
 299 (DSI) have become progressively widespread in GSA applications across different  
 300 hydrological modelling fields (e.g. Pappenberger *et al.*, 2008; Peeters *et al.*, 2014). In the  
 301 DSI approach proposed by Pianosi and Wagener (2015) which is named PAWN (derived  
 302 from the authors names), the model output distribution for  $t_{SHF}$  is characterized by a data  
 303 sample Cumulative Density Function (CDF) rather than its Probability Density Function  
 304 (PDF). Practically, in the PAWN indices, the sensitivity to input  $x_i$  is measured by the  
 305 distance between the empirical unconditional CDF of output  $t_{SHF}$ ,  $\hat{F}_{t_{SHF}}(t_{SHF})$  that is  
 306 obtained when all inputs vary simultaneously, and the empirical conditional CDF,  
 307  $\hat{F}_{t_{SHF}|x_i}(t_{SHF})$  that are obtained when varying all inputs but  $x_i$  is fixed at a nominal  
 308 value, through the Kolmogorov-Smirnov statistic,  $\widehat{KS}$  (Kolmogorov, 1933):

$$\widehat{KS}(x_i) = \max_{t_{SHF}} |\hat{F}_{t_{SHF}}(t_{SHF}) - \hat{F}_{t_{SHF}|x_i}(t_{SHF})| \quad (20)$$



309 Figure 4 shows the  $\widehat{KS}$  obtained from the empirical unconditional and conditional CDFs.  
 310 The empirical unconditional CDF  $y$ ,  $\widehat{F}_{t_{SHF}}(t_{SHF})$  is approximated using  $N_u$  output  
 311 estimations obtained by sampling the entire input feasibility region. The conditional CDF  
 312  $t_{SHF}$ ,  $\widehat{F}_{t_{SHF}|x_i}(t_{SHF})$  is approximated using  $N_c$  output estimations obtained by sampling  
 313 the non-fixed inputs only, while the value of  $x_i$  is kept fix. As statistics  $KS$  depends on  
 314 the value at which  $x_i$  fixed, the index  $\widehat{T}_i$  considers the maximum values of  $\widehat{KS}$  over all  
 315 possible values of  $x_i$  (Pianosi and Wagener, 2015):

$$\widehat{T}_i = \max_{x_i = \bar{x}_i^{(1)}, \bar{x}_i^{(2)}, \dots, \bar{x}_i^{(n)}} |\widehat{KS}(x_i)| \quad (21)$$

316 where  $\bar{x}_i^{(1)}, \bar{x}_i^{(2)}, \dots, \bar{x}_i^{(n)}$  are randomly sampled values for the fixed input  $x_i$ . The lower  
 317 value of  $\widehat{T}_i$ , ( $\widehat{T}_i \in [0,1]$ ) indicates the lower influence of the corresponding  $x_i$  on  $t_t$ . The  
 318 total number of model evaluations necessary to compute the sensitivity index  $\widehat{T}_i$  for all  
 319 the  $N_{param}$  inputs is  $N_u + n' \times N_c \times N_{param}$  where  $N_u$ ,  $n'$ , and  $N_c$  are the number of  
 320 samples to estimate the unconditional CDF, conditional CDF, and condition points,  
 321 respectively. The proper values for  $n'$ ,  $N_u$  and  $N_c$  can be selected by trial-and-error to  
 322 follow regularity properties of CDFs (continuity, monotonicity, relative smoothness). The  
 323 index  $\widehat{T}_i$  is a global, model-independent, robust, quantitative, dimensionless, with no need  
 324 for parameter tuning, no computing costs for computing the CDF, easy to implement,  
 325 facilitates the application of bootstrapping and convergence analysis, and is unconditional  
 326 on any assumed input value (Pianosi *et al.* 2015). In this study, the sensitivity index  
 327 ( $\widehat{KS}(x_i)$  and  $\widehat{T}_i$ ) of the sheet-flow travel time ( $t_{SHF}$ ) estimated by K-M and K-D  
 328 formulations to the input parameters of flow temperature ( $T$ ), roughness ( $f$  or  $n$ ), surface  
 329 slope ( $S$ ), rainfall depth ( $P$ ), rainfall duration ( $D$ ), average rainfall depth ( $P_{24}$ ), runoff-  
 330 coefficient ( $C$ ), and length of plane surface ( $L$ ) are calculated using Eq. 8. Whereas the  
 331 input parameters related to NRCS storm characteristics are considered according to

332 Froehlich (2009). The index  $\hat{T}_i$  is a helpful tool to investigate the relative influence of  
 333 model parameters on predictive accuracy as well as to understand the dominant factors  
 334 which control the precision of  $t_{SHF}$ .

335

#### 336 4. Results and Discussion

337 The cumulative density function (CDF) of  $\hat{F}_{t_{SHF}}(t_{SHF})$  and  $\hat{F}_{t_{SHF}|x_i}(t_{SHF})$  for the model  
 338 output ( $t_{SHF}$ ) for the wide range of eight influenced parameters of K-M formulation with  
 339 zero-upstream boundary condition ( $n, S, D, P, \lambda, CN, P_{24}, L$ ) and also for nine effective  
 340 parameters of K-D formulation ( $T, f, S, D, P, \lambda, CN, P_{24}, L$ ) are computed (the results are  
 341 not shown). The CDFs of all parameters grow significantly away from their initial  
 342 uniform distributions but in different ways which lead to different sensitivity to these  
 343 parameters. The sensitivity index of  $\widehat{KS}(x_i)$  for the influential parameters in the  
 344 estimation of  $t_{SHF}$  by K-D and K-M formulations are shown in Fig. 5 where  $\alpha=0.05$ ,  
 345  $n' = 10$ ,  $N_u = 100$ , and  $N_c = 50$ . In both formulations, the effect of the temporal  
 346 distribution of storm intensity is investigated by incorporating four temporal rainfall  
 347 distributions of NRCS. The values of  $\widehat{KS}(x_i)$  indicate that the storm occurrence time (e.g.  
 348 winter or spring) are not affected by the  $t_{SHF}$  estimated by K-D formula since all values  
 349 of this index rely on below critical values for a wide range of the flow temperature  
 350 (between 2 to 45 °C) as shown in Fig. (5-a). In addition, the  $t_{SHF}$  estimated by both  
 351 formulations of K-D and K-M are not significantly sensitive to the wide range of rainfall  
 352 depth,  $P$  (ranging from 0 to 1000 mm), initial abstraction ratio,  $\lambda$  (ranged 0.001 to 0.8),  
 353 and also curve number,  $CN$  (ranging from 30 to 99) for all types of NRCS storms (except  
 354 to  $P < 100$  mm of NRCS Type II in K-M formula) (Figs. 5 (e-g) and (m-o)). According to  
 355 Eq. 17, the parameters  $P$ ,  $\lambda$ , and  $CN$  contribute to the calculation of runoff coefficient,  $C$ ,  
 356 which is apparently not a significantly influential parameter on  $t_{SHF}$ . It should be noted

357 that the values of  $\widehat{KS}$  indicate the relative influence of the corresponding parameter in  
358 comparison with other influential parameters. Further investigations indicate that  
359 computing the  $\widehat{KS}$  for the input parameters of K-D and K-M formulae by directly entering  
360 the parameter  $C$  into Eq. 16 (in the range of 0.05 to 0.95), show that  $t_{SHF}$  is significantly  
361 sensitive to lower and upper values of  $C$  ( $<0.15$  or  $>0.80$ ) for all NRCS storms as shown  
362 in Fig. 6. However, the sensitivity of  $t_{SHF}$  to the lower and upper ranges of parameter  $C$   
363 through K-M formula is greater than K-D. According to FWHA (1996), the lower values  
364 of  $C$  correspond to lawns with sandy soil and un-improved natural area (e.g. forest),  
365 whereas the upper values correspondent to asphaltic and concrete area in developed urban  
366 watersheds (e.g. rooftops, parking lots, and paved surfaces). Results of the  $\widehat{KS}$   
367 corresponding to both K-M and K-D formulations indicate that  $t_{SHF}$  is not influenced by  
368  $C$  over the areas with intermediate values of runoff coefficient ( $0.2 < C < 0.8$ ). For the  
369 upper values of  $C$ , the effect of temporal rainfall distribution (i.e. NRCS storms) is more  
370 dominant than for lower values.

371 The  $t_{SHF}$  is influenced by flow resistance (parameter  $f$  in K-D and parameter  $n$  in K-M  
372 formulae) for lower ( $f < 10$  and  $n < 0.22$ ) and upper ( $f > 50$  and  $n > 0.6$ ) values of surface  
373 roughness as shown in Figs. (5-b and 5-j). According to Engman (1986), the lower values  
374 of  $n$  correspond to asphalt and concrete, bare soil, and natural rangeland areas whereas  
375 the upper values link to the surfaces covered with dense grass. Interestingly, the  
376 sensitivity of the  $t_{SHF}$  estimated by K-D and K-M formulae to lower values of flow  
377 resistance is similar for four types of NRCS storms. However, the effect of temporal  
378 rainfall distribution is dominant for very rough surfaces. The intermediate rough surfaces  
379 (i.e.  $0.2 < n < 0.6$ ) do not have a significant influence on the  $t_{SHF}$ , despite the dominance of  
380 temporal rainfall distribution for these surfaces. Surface plane slope ( $S$ ) less than 10% (or  
381  $6^\circ$ ) has a significant influence on the estimation of  $t_{SHF}$  by two formulations of K-M and

382 K-D (Figs. 5-c and 5-k). This surface slope is frequently observed in natural watersheds  
383 (except to steep hill slopes which may be unstable) and also for the design of transverse  
384 slopes of roads (FHWA 1984).

385 The meaningfulness of the rainfall duration ( $D$ ) on the  $t_{SHF}$  estimated by K-M and K-D  
386 formulae is limited to  $D < 180 \text{ min}$  (or  $6 \text{ hr}$ ) for all types of NRCS storms. Storms with a  
387 duration greater than  $6 \text{ hr}$  do not have a significant impact on the  $t_{SHF}$  due to the  
388 decreasing storm intensity according to  $i - D$  relations. The  $t_{SHF}$  is influenced  
389 significantly by 2-years 24-hr rainfall depth for  $P_{24} < 200 \text{ mm}$  or  $P_{24} > 800 \text{ mm}$  for both  
390 formulations of K-M and K-D and different types of NRCS storms (Figs. 5-h and 5-p).  
391 The range of  $P_{24} < 200 \text{ mm}$  covers the 2-years daily rainfall depth for all types of NRCS  
392 design storms in USA (SCS 1986).

393 The significant effect of surface plane length ( $L$ ) on the estimation of  $t_{SHF}$  by the K-D  
394 and K-M formulations is limited to about  $L < 3500 \text{ m}$  (Figs. 5-I and 5-q). Noting the  
395 constraint of  $100 \text{ m}$  (or  $300 \text{ ft}$ ) for sheet-flow length by TR-55, this parameter plays an  
396 important role in the  $t_{SHF}$  over a wide range of surfaces in natural and urban watersheds.

397 According to Eq. 18, the sensitivity index  $\hat{T}_i$  is calculated as the maximum value of  $\widehat{KS}$   
398 over all possible values of input parameters in the K-M and K-D formulations (see Fig.

399 7). This index can be beneficial for ranking the sensitivity of the parameters that  
400 influence  $t_{SHF}$  for different storm types. Results of Fig. 7 reveal the dominant influence

401 of parameter  $L$  in the estimation of  $t_{SHF}$  by K-M and K-D formulae and also for all types  
402 of NRCS storms, except in the case of NRCS Type II and K-M formula where the

403 parameter  $n$  has the greatest influence. After the parameter  $L$ , the order of index  $\hat{T}_i$   
404 changes for K-M and K-D formulations and also for NRCS design storms. For all types

405 of NRCS storms, the  $t_{SHF}$  estimated by K-M has the minimum sensitivity to the flow  
406 temperature. However, the  $t_{SHF}$  estimated by both formulations indicate lower sensitivity

407 to the parameters of the SCS-CN model (i.e.  $\lambda$ ,  $CN$ , and  $P$  according to Eq. 17), but  
408 incorporating the runoff coefficient ( $C$ ) directly in the models results in a significant  
409 increase of  $\hat{T}_i$  related to this parameter (0.35 for K-D and 0.4 to 0.5 for K-M). On  
410 average, the two formulations of K-D and K-M consistently indicate that the plane  
411 surface characteristics (i.e.  $n$  or  $f$ ,  $CN$ ,  $L$ , and  $S$ ) have the greater impacts on the  $t_{SHF}$  ( $\hat{T}_i$   
412 = 0.43 and 0.41, respectively) in comparison to storm and climate characteristics (i.e.  $T$ ,  
413  $D$ ,  $\lambda$ ,  $P$ , and  $P_{24}$ ) ( $\hat{T}_i = 0.20$  and  $0.27$ , respectively) for all NRCS storms. The surface  
414 related parameters have a near equal influence on  $t_{SHF}$ , whereas in the K-M formula,  
415 there is higher sensitivity to the parameters related to storm and climate. In addition, the  
416 order of average sensitivity of the  $t_{SHF}$  on the input parameters of K-D and K-M formulae  
417 are associated with the NRCS Type II ( $\hat{T}_i = 0.33$  and  $0.40$ ), I, III, and then Type Ia,  
418 respectively. Table 2 summarizes the values of flow resistance coefficients ( $\tau_1$ ,  $\tau_2$ ,  $\tau_3$ ,  
419 and  $n$ ) for three surfaces of grass, concrete, and turf used for estimation of the  $t_{SHF}$  by the  
420 four formulae which were obtained from previous experiments.

421 It should be mentioned that the values of  $\tau_1$ ,  $\tau_2$ ,  $\tau_3$ , and  $n$  in Table 2 are based on  
422 selected parameters (e.g. surface slope, rainfall intensity, surface roughness) that were  
423 adopted in the application examples. The flow resistance coefficients need revision due to  
424 complicated dynamics of flow resistance caused by the influential factors (Saghafian and  
425 Julien 1989).

426

## 427 **5. Application of Formulae**

428 Twenty sets of experimental data covering a wide range of the influential factors (i.e.  $L$ ,  
429  $S$ ,  $i_e$ , and  $n$ ) on the measured  $t_{SHF}$  over a single plane surface are collected from  
430 previous studies and used to illustrate the performance of the developed formulations.  
431 Table 2 indicates the source experimental data, observed values of  $t_{SHF}$  and also  $t_{SHF}$

432 values estimated using the K-M formula in two conditions  $q_u = q_d$  (so-called K-M1) and  
433  $q_u=0$  (so-called K-M2), and K-D formula. For these experimental data, the TR-55  
434 formula cannot be used due to lack of available information of  $P_{24}$  values. Results of  
435 Table 2 indicate that the calculated goodness of fit criteria  $\eta$  (obtained by using Eq. 13 or  
436 14) and  $N_{K-W}$  indicates that all values of  $\eta$  and  $N_{K-W}$  are significantly greater and  
437 smaller than threshold value of 50 and 100, respectively. This guarantees that the K-W  
438 theory provides a very good approximation for all cases shown in Table 2. Considering  
439 zero-upstream boundary condition (assumed by K-M1 formula) are more realistic as flow  
440 runs over the single plane rather than the assumption of uniform flow depth all over the  
441 surface plane. For this purpose, the average percentage of error (APE) for three formulae  
442 of K-M1, K-M2, and K-D and for different flow regimes downgradient of the surface  
443 plane are computed and shown in Fig. 8. This assumption resulted in a reduction of APE  
444 in the estimation of  $t_{SHF}$  as 22.17%, 26.27%, and 18.90% for laminar, transitional, and  
445 turbulent flow regime, respectively. It is noteworthy that incorporating the Darcy-  
446 Weisbach friction in K-W theory (i.e. K-D formula) outperforms K-M1 and K-M2,  
447 especially for laminar and turbulent sheet-flow regimes. However, in transitional flow  
448 regime, the APE values for K-D and K-M2 are close together (6.03% and 6.39%,  
449 respectively), but the K-D indicates significant improvement for laminar and turbulent  
450 flow regime (6.4% and 5.67%, respectively).

451 It is noteworthy that among the used experimental data, the minimum APE value in the  
452 estimation of the  $t_{SHF}$  by three formulae is obtained in the cases of having the transitional  
453 and laminar flow regimes downgradient in the surface plane (Fig. 8). Three formulae  
454 have the maximum error in estimation of  $t_{SHF}$  for turbulent flow regime downgradient in  
455 the plane. Despite the fact that the Manning based formulae (i.e. K-M1 and K-M2) is  
456 based on the assumption of occurring turbulent flow regime over the whole surface plane,

457 the K-D formula is also proficient (i.e. less APE value) in this flow-regime condition.  
458 Underestimation of  $t_{SHF}$  by three formulae, especially when the sheet-flow regime is  
459 turbulent (see the calculated values of  $t_{SHF}$  in Table 2), may lead to the overestimation of  
460 peak discharge in the hydrological design. These findings imply that considering one type  
461 of flow regime (i.e. turbulent) throughout the surface plane, as is the case with the  
462 Manning based formulae, could not be relied on to coincide with the realistic hydraulic  
463 condition of sheet-flow. Previous research works (i.e. Bulter, 1977; Singh, 1988; Chen  
464 and Wong, 1993) reported the inevitability of laminar or transitional flow regimes  
465 occurring before turbulent flow regime as sheet-flow moves downgradient of the surface  
466 plane which leads to increasing the  $t_{SHF}$ . Moreover, uncertainties and data scarcity of  
467 friction factor  $f$  for different flow regimes and surface types are likely reasons why  $t_{SHF}$   
468 is underestimated by K-D formula.

469 The performance of the K-M and K-D formulae in the estimation of  $t_{SHF}$  are also  
470 compared over hillslope-riparian-stream hydrologic connectivity system as multiple  
471 continuous planes (MCPs). Unfortunately, no previous experimental data is available to  
472 assess the  $t_{SHF}$  over MCPs. For the purpose of intercomparison of two K-M and K-D  
473 formulae, a continuous cascade of three surfaces are assumed as a grassy surface at up-  
474 gradient plane (covered by Kentucky blue grass), a smooth surface at middle plane (e.g.  
475 rooftops, parking lot, and paved surfaces such as streets), and a slightly rough surface (i.e.  
476 turf) at down-gradient plane. For the real-world application of the results, the surface  
477 planes and storm and climate characteristics in these examples were collected from the  
478 previous studies. The effect of temporal distributions of rainfall is also investigated by  
479 considering four NRCS Type I, Ia, II, and III. The flow resistance parameters ( $\tau_1$ ,  $\tau_2$ , and  
480  $\tau_3$ ), Manning's roughness coefficient ( $n$ ), and runoff coefficient ( $C$ ) of three considered  
481 surfaces are given in Table 2. These parameters are kept constant for the corresponding



482 surfaces in all analysis. The values of  $t_{SHF}$  by two formulae (K-M and K-D) are  
483 calculated by considering numerous sets of input parameters (some of the results are  
484 shown in Table 4).

485 For each case, the percentage of turbulent flow portion on the three surfaces and the  
486 absolute difference of two formulations in the estimation of  $t_{SHF}$  are also calculated and  
487 given in Table 4. Results shown in Table 4 can be summarized as follows:

488 1) In all cases, the estimated values of  $t_{SHF}$  by the K-D formula are greater than those  
489 obtained by the K-M3 approach due to incorporating the effects of three flow regimes  
490 (laminar, transitional, and turbulent) in K-D formula instead of turbulent flow only.  
491 Longer  $t_{SHF}$  leads to delaying the time of peak flow and thus, changes the shape of the  
492 unit hydrograph obtained by two formulae.

493 2) A significant inverse correlation between the difference of K-M3 and K-D results and  
494 the portion of turbulent flow regime over the surfaces of planes is observed when the  
495 NRCS storm Type I, II, and III is considered. A weak correlation between two  
496 formulations of K-D and K-M3 is observed when the NRCS storm Type Ia is applied.

497 3) Changing the sheet-flow temperature due to weather conditions and rainy season  
498 affects the  $t_{SHF}$  estimated by K-D formula, whereas the K-M3 formula cannot incorporate  
499 the changes in flow temperature. This is one of the disadvantages of Manning based  
500 formulations.

501 4) The estimated values of  $t_{SHF}$  over multi-planar surfaces by K-D and K-M3 formulae  
502 are also affected by the sequence of the planes. If the sequence of planes in the sheet-flow  
503 direction is grassy area-concrete-turf (G→C→T) the  $t_{SHF}$  obtained by the K-D and also  
504 K-M3 formulae are different from other surface arrangement (e.g. G→T→C or  
505 C→T→G). The gradual increase of flow resistance (or decrease of runoff coefficient) in  
506 direction of sheet-flow over the cascade of surface planes leads to the two formulations



507 giving close results and less travel time than other sequences of surfaces (see rows #1, 8,  
508 and 9 in Table 3).

509 5) The calculated values of the  $t_{SHF}$  through NRCS storm Type Ia and Type II produces  
510 the maximum and minimum values of  $t_{SHF}$ , respectively.

511 6) Since the TR-55 formula uses 2-years  $P_{24}$  for the excess rainfall intensity ( $i_e$ ), the  
512 same results are estimated using this formula when  $P_{24}$  is constant even if rainfall  
513 intensities change significantly (i.e. different NRCS storms).

514

## 515 6. Conclusion

516 • For small watersheds in which sheet-flow is the major contributor (or possibly the  
517 only contributor) to the time of concentration of watershed, the difference in  
518 estimation of  $t_{SHF}$  made when using various K-W based formulations likely have a  
519 considerable influence on peak-flow estimation and hence the appropriate design of  
520 drainage structures. The results obtained from GSA demonstrated that the main  
521 controlling parameters of  $t_{SHF}$  over the single plane and cascade of multiple planes  
522 estimated by K-M and K-D formulae are flow resistance, length of the surface plane,  
523 surface slope, and excess rainfall intensity. Conversely, the lowest sensitivity of  $t_{SHF}$   
524 in K-D formula is to flow viscosity. This implies  $t_{SHF}$  is not affected by the weather  
525 temperature if the other influential parameters are kept constant.

526 • Results of this study indicate that the kinematic Darcy-Weisbach formulation (K-D)  
527 outperforms the kinematic Manning (K-M) formula in the estimation of  $t_{SHF}$  due to  
528 the fact that it considers the variations of flow regime on the surface plane. The  
529 developed formulae in this study maybe serve in the structure of stormwater  
530 hydrological models (e.g. TR-55 and HydroCAD) to have appropriate estimation of  
531  $t_{SHF}$  in urban and small watersheds, and therefore increase confidence in design peak

532 discharge and drainage structure sizes for the required level of risk. Despite the fact  
533 that a more precise estimation of  $t_{SHF}$  would be obtained using the K-D formula over  
534 the single plane surface, of the lack of available data and also uncertainties associated  
535 with the friction factor ( $f$ ) for different flow regimes and surface roughness is a  
536 significant challenge with the application of this formula.

537 • Overestimation of peak discharge may occur in hydrological forecasting and design  
538 due to use of shorter estimates of  $t_{SHF}$  estimated by both Manning- and Darcy-  
539 Weisbach-based formulae.

540 • The estimated  $t_{SHF}$  by two formulations of kinematic Manning (K-M3) and K-D over  
541 the cascade of continuous planes is also affected by the sequence of the planes due to  
542 change in upstream flow boundary condition.

543 The kinematic wave approximation of Saint-Venant equations obtained by the method of  
544 characteristics is analytic, computationally efficient, considers the effects of flow regime  
545 over multiple planes and accurate rainfall intensity in estimation of travel time of sheet-  
546 flow in one dimension. More accurate results can be obtained with employing a  
547 physically based fully-distributed numerical model that are more realistic, avoiding the  
548 simplifications, considering the spatial heterogeneity of data, and also the effect of more  
549 flow components (i.e. transverse and depth flow directions).

550

## 551 **Acknowledgements**

552 The authors appreciate the constructive comments of the Editor-in-Chief Dr. Geoff Syme  
553 and anonymous reviewers that helped to improve the final version of this paper. The  
554 authors Behzad Ataie-Ashtiani and Craig T. Simmons acknowledge support from the  
555 National Centre for Groundwater Research and Training, Australia. Behzad Ataie-

556 Ashtiani appreciates the support of the Research office of the Sharif University of  
 557 Technology, Iran.

558

559 **Nomenclature**

$\widehat{KS}$ [-]	Kolmogorov-Smirnov statistic
CN [-]	Curve number
$C$ [-]	Runoff coefficient
$D$ [T]	Rainfall duration
$I$ [ $L T^{-1}$ ]	Infiltration rate
$L$ [L]	Length of surface plane in direction of sheet-flow
$N$ [-]	Number of planes in sheet-flow direction
$P$ [L]	Rainfall depth
$R$ [L]	Direct runoff depth
$S$ [ $L L^{-1}$ ]	Slope of surface plane in flow direction (bed slope)
$V$ [ $L T^{-1}$ ]	Average velocity of sheet-flow
$V$ [ $L T^{-1}$ ]	Sheet-flow velocity at any point
$W$ [L]	Width of sheet-flow
$a'$ [-]	Constant of rainfall intensity-duration relation
$b'$ [-]	Constant of rainfall intensity-duration relation
$f$ [-]	Darcy-Weisbach friction
$g$ [ $L T^{-2}$ ]	Acceleration due to gravity
$i$ [ $L T^{-1}$ ]	Average of total rainfall intensity
$n$ [ $L^{-1/3} T$ ]	Manning's roughness coefficient
$n'$ [-]	Number of samples to estimate condition points
$q$ [ $L^2 T^{-1}$ ]	Unit discharge of sheet-flow
$t$ [T]	Time since excess rainfall appears
$x$ [L]	Distance along the plane in flow direction
$y$ [L]	Depth of sheet-flow perpendicular to plane surface

$\hat{F}_{t_{SHF}}(t_{SHF}) [-]$	Empirical unconditional CDF of $t_{SHF}$
$\hat{F}_{t_{SHF} x_i}(t_{SHF}) [-]$	Empirical conditional CDF of $t_{SHF}$
$\hat{T}_i [-]$	Maximum values of $\widehat{KS}$
$L_1 [L]$	Portion of plane length with laminar flow
$L_2 [L]$	Portion of plane length with transitional flow
$L_3 [L]$	Portion of plane length with turbulent flow
$N_c [-]$	Number of samples to estimate conditional CDF
$N_u [-]$	Number of samples to estimate unconditional CDF
$P_{24} [L]$	24-hr rainfall depth
$R_h [L]$	Hydraulic radius of sheet-flow
$R_e [-]$	Reynolds number
$Re_1 [-]$	Critical Reynolds numbers to have laminar flow
$Re_2 [-]$	Critical Reynolds numbers to have transitional flow
$S_f [L L^{-1}]$	Friction slope
$V_{max} [L T^{-1}]$	Sheet-flow velocity at downstream edge of surface
$i_e [L T^{-1}]$	Average of excess rainfall intensity
$q_d [L^2 T^{-1}]$	Unit discharge of sheet-flow at downstream edge of surface
$q_u [L^2 T^{-1}]$	Unit discharge of sheet-flow at upstream edge of surface
$t_1 [T]$	Sheet-flow travel time for laminar flow portion
$t_2 [T]$	Sheet-flow travel time for transitional flow portion
$t_3 [T]$	Sheet-flow travel time for turbulent flow portion
$t_{SHF} [T]$	Sheet-flow travel time
$y_d [L]$	Sheet-flow depth at upstream edge of surface
$y_{max} [L]$	Sheet-flow depth at downstream edge of surface
$y_u [L]$	Sheet-flow depth at upstream edge of surface
$x_i [-]$	Input parameters to model
$\tau_1 [-]$	Constant value that related $R_e$ to $f$ in laminar flow regime
$\tau_2 [-]$	Constant value that related $R_e$ to $f$ in transitional flow regime

$\tau_3$ [–]	Constant value that related $R_e$ to $f$ in turbulent flow regime
$\alpha$ [–]	Coefficient of Darcy-Weisbach friction formula
$\beta$ [–]	Coefficient of Darcy-Weisbach friction formula
$\gamma$ [–]	Conversion factor of units
$\delta$ [–]	Constant value equal to $3.6 \times 10^6$
$\lambda$ [–]	Initial abstraction ratio
$\nu$ [ $L^2 T^{-1}$ ]	Kinematic viscosity of sheet-flow
$\omega$ [ $L T^{-1}$ ]	Celerity of the wave

560

561 **References**

- 562 Agiralioglu, N., 1985. Analytical solution of leaf-shaped basin flow. Hydrological  
563 Sciences Journal, 30(3), 407–424. <https://doi.org/10.1080/02626668509491003>
- 564
- 565 Akan, A. O., 1986. Time of concentration of overland flow. J. Irrig. and Drain. Engrg.,  
566 ASCE, 112(4), 283-292. [https://doi.org/10.1061/\(ASCE\)0733-9437\(1986\)112:4\(283\)](https://doi.org/10.1061/(ASCE)0733-9437(1986)112:4(283))
- 567 ASCE, 1992. Design and construction of urban stormwater management systems: ASCE  
568 manuals and reports of engineering practice no. 77. New York.
- 569 Baroni, G., and Tarantola, S., 2014. A general probabilistic framework for uncertainty and global  
570 sensitivity analysis of deterministic models: a hydrological case study. Environ. Model. Softw.  
571 51, 26-34. <https://doi.org/10.1016/j.envsoft.2013.09.022>
- 572 Beldring, S., Gottschalk, L., Rodhe, A, and Tallaksen, L.M., 2000. Kinematic wave  
573 approximations to hillslope hydrological processes in tills. Hydrol. Process. 14, 727-  
574 745. [https://doi.org/10.1002/\(SICI\)1099-1085\(200003\)14:4<727::AID-HYP969>3.0.CO;2-D](https://doi.org/10.1002/(SICI)1099-1085(200003)14:4<727::AID-HYP969>3.0.CO;2-D)
- 575 Ben-zvi, A. 1984. Runoff peaks from two-dimensional laboratory watersheds. Journal of  
576 Hydrology, 68(1–4), 115-139. [https://doi.org/10.1016/0022-1694\(84\)90207-5](https://doi.org/10.1016/0022-1694(84)90207-5)
- 577 Brakensiek, D.L., 1967. Kinematic flood routing. Transactions of the American Society  
578 of Agricultural Engineers, 10(3), 340–343.
- 579 Bulter, S.S., 1977. Overland-flow travel time versus Reynolds number. J. Hydro., 32,175-  
580 182. [https://doi.org/10.1016/0022-1694\(77\)90125-1](https://doi.org/10.1016/0022-1694(77)90125-1)
- 581 Cahill, A., and Li, M.H., 2003. Measurement and simulation of flow on surface with  
582 extreme low slope for determination of time of concentration. Report 0-4404-2,

- 583 Performed in cooperation with the Texas Department of Transportation and the  
584 Federal Highway Administration, October 2003.
- 585 Campbell, S.Y., Parlange, J.Y., and Rose, C.W., 1984. Overland flow on converging and  
586 diverging surfaces: kinematic model and similarity solutions. *J. Hydro.* 70, 367–374.  
587 [https://doi.org/10.1016/0022-1694\(84\)90252-X](https://doi.org/10.1016/0022-1694(84)90252-X)
- 588 Chen, C. N., and Evans, R. R., 1977. Application of kinematic wave method to predict  
589 overland peak flows. *Proc. Int. Sym. on Urban Hydro., Hydr., and Sediment Control*,  
590 Univ. of Kentucky, Lexington, Ky., 113-118.
- 591 Chen, C., 1976. Flow resistance in broad shallow grassed channels, *Journal of the*  
592 *Hydraulic Division, ASCE*, 102, HY3, 307-322.
- 593 Crandall, S.H., 1956. *Engineering analysis*: New York, McGraw Hill, 417 p.
- 594 Cronshey, R.G. and Woodward, D.E., 1989. Derivation of the Type III rainfall  
595 distribution, paper presented at the International Conference on Channel Flow and  
596 Catchment Runoff. Charlottesville, VA, International Association for Hydraulic  
597 Research.
- 598 Dewberry, V.A., 2003. Research on Appropriateness of Travel Time Calculations in  
599 Coastal Plain Watersheds. Report submitted to Gloucester County Soil Conservation  
600 District, New Jersey, and New Jersey Department of Agriculture, State Soil  
601 Conservation Committee.
- 602 Eagleson, P.S., 1970. *Dynamic hydrology*. McGraw-Hill, New York, N.Y.
- 603 Engman, E.T., 1986. Roughness coefficients for routing surface runoff. *J. Irrig. and*  
604 *Drain. Engrg.*, ASCE, 112(1), 39-53. [https://doi.org/10.1061/\(ASCE\)0733-](https://doi.org/10.1061/(ASCE)0733-9437(1986)112:1(39))  
605 [9437\(1986\)112:1\(39\)](https://doi.org/10.1061/(ASCE)0733-9437(1986)112:1(39))
- 606 Fenzel, R.N., and Davis, J.R., 1964. Hydraulic resistance relationships for surface flows  
607 in vegetated channels, *Trans., ASAE*, 7, 46-51.
- 608 Froehlich, D.C., 2009. NRCS design storm erosivity. *Journal of Irrigation and Drainage*  
609 *Engineering, ASCE*, 135(1), 76–86. [https://doi.org/10.1061/\(ASCE\)0733-](https://doi.org/10.1061/(ASCE)0733-9437(2009)135:1(76))  
610 [9437\(2009\)135:1\(76\)](https://doi.org/10.1061/(ASCE)0733-9437(2009)135:1(76))
- 611 Froehlich, D.C., 2011. NRCS overland flow travel time calculation. *Journal of Irrigation*  
612 *and Drainage Engineering, ASCE*, 137(4), 258-262.  
613 [https://doi.org/10.1061/\(ASCE\)IR.1943-4774.0000287](https://doi.org/10.1061/(ASCE)IR.1943-4774.0000287)
- 614 García-Serrana, M., Gulliver, J.S., Nieber, J.L., 2017. Non-uniform overland flow-  
615 infiltration model for roadside swales. *Journal of Hydrology* 552, 586–599.

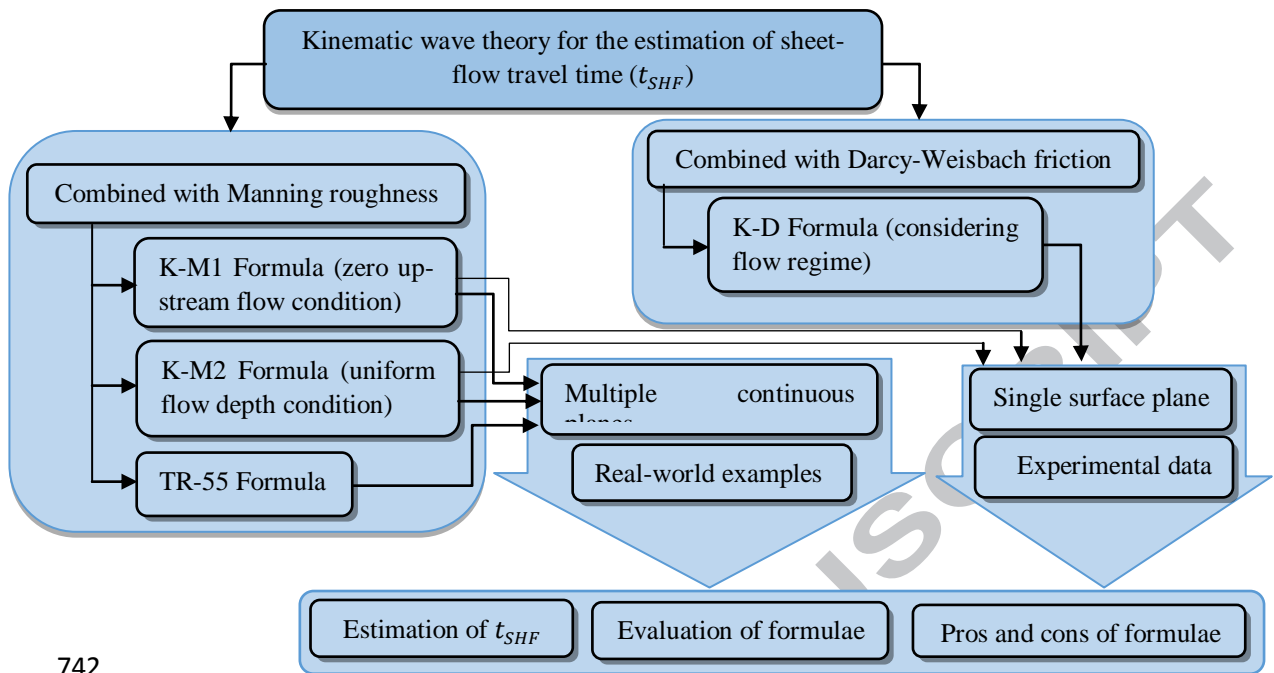
- 616 Grismer, M.E., 2016. Surface runoff in watershed modeling—turbulent or laminar flows?  
617 Hydrology, 3(18). <https://doi.org/10.3390/hydrology3020018>
- 618 Hawkins, R.H., 1983. Relation between curve number and runoff coefficient. J. Irrig.  
619 Drain Eng., ASCE, 109, 192-195.
- 620 Henderson, F.M., and Wooding, R.A., 1964. Overland flow and ground-water flow from  
621 a steady rainfall of finite duration: Journal of Geophysical Research, 69(8), 1531-  
622 1540.
- 623 Hessel, R., Jetten, V., and Guanghui, Zh., 2003. Estimating Manning's n for steep slopes.  
624 Catena, 54, 77–91. [https://doi.org/10.1016/S0341-8162\(03\)00058-4](https://doi.org/10.1016/S0341-8162(03)00058-4)
- 625 Izzard, C.F., 1944. The surface profile of overland flow, Trans., American Geophys.  
626 Union, 25, 950-968.
- 627 Julien, P.Y., and Simons, D.B., 1985. Sediment transport capacity of overland flows,  
628 Trans. Am. Soc. Agric. Eng., 28(3), 755-762.
- 629 Kibler, D.F., and Woolhiser, D.A., 1970. The kinematic cascade as a hydrologic model:  
630 Colorado State University, Hydrology Paper No. 39, 28 p.
- 631 Langford, K.J., and Turner, A.K. 1973. An experimental study of the application of  
632 kinematic wave theory to overland flow. Journal of Hydrology, 18, 125 - 145.  
633 [https://doi.org/10.1016/0022-1694\(73\)90099-1](https://doi.org/10.1016/0022-1694(73)90099-1)
- 634 Lighthill, M.J., and Whitham, G.B., 1955. On kinematic waves, I. Flood movement in  
635 long rivers: Proceedings of the Royal Society, Series A, 229, 281-316.
- 636 McCuen R.H. and Okunola, O., 2002. Extension of TR-55 for Microwatersheds. ASCE  
637 Journal of Hydrologic Engineering, 7(4), 319-325. [https://doi.org/10.1061/\(ASCE\)1084-  
638 0699\(2002\)7:4\(319\)](https://doi.org/10.1061/(ASCE)1084-0699(2002)7:4(319))
- 639 McCuen, R.H. and Spiess, J.M. 1995. Assessment of kinematic wave time of  
640 concentration. Journal of Hydraulic Engineering, 121(3), 256-266.  
641 [https://doi.org/10.1061/\(ASCE\)0733-9429\(1995\)121:3\(256\)](https://doi.org/10.1061/(ASCE)0733-9429(1995)121:3(256))
- 642 McCuen, R.H., Wong, S.L., and Rawls, W.J., 1984. Estimating urban time of  
643 concentration. Journal of Hydraulic Engineering, 110(7), 887-904.  
644 [https://doi.org/10.1061/\(ASCE\)0733-9429\(1984\)110:7\(887\)](https://doi.org/10.1061/(ASCE)0733-9429(1984)110:7(887))
- 645 Miller, J.E., 1983. Basic concepts of kinetic-wave models. United States Department of  
646 the Interior, Geological Survey professional paper, No. 1302.
- 647 Miller, W.A., and Cunge, J.A., 1975. Simplified equations of unsteady flow, in  
648 Mahmood, K., and Yevjevich, V., eds., Unsteady flow in open channels: Water  
649 Resources Publications, p. 183-249.

- 650 Natural Resources Conservation Service (NRCS), 1986. Urban hydrology for small  
651 watersheds. Technical Release 55, 2nd Ed., U.S. Dept. of Agriculture, Washington,  
652 DC.
- 653 Overton, D.E., and Meadows, M.E., 1976. Stormwater modeling. Academic Press, New  
654 York, N.Y.
- 655 Pappenberger, F., Beven, K., Ratto, M., and Matgen, P., 2008. Multi-method global  
656 sensitivity analysis of flood inundation models. *Adv. Water Resour.* 31 (1), 1-14.  
657 <https://doi.org/10.1016/j.advwatres.2007.04.009>
- 658 Peeters, L.J.M., Podger, G.M., Smith, T., Pickett, T., Bark, R.H., and Cuddy, S.M., 2014. Robust  
659 global sensitivity analysis of a river management model to assess nonlinear and interaction  
660 effects. *Hydrol. Earth Syst. Sci.*, 18(9), 3777–3785. <https://doi.org/10.5194/hess-18-3777-2014>
- 661 Phelps, H.O., 1970. The friction coefficient for shallow flows over a simulated turf  
662 surface. *Water Resources Research*, 6(4), 1220-1226.  
663 <https://doi.org/10.1029/WR006i004p01220>
- 664 Pianosi, F., and Wagener, T., 2015. A simple and efficient method for global sensitivity  
665 analysis based on cumulative distribution functions. *Environmental Modelling &  
666 Software* 67, 1-11. <https://doi.org/10.1016/j.envsoft.2015.01.004>
- 667 Pianosi, F., Sarrazin, F., and Wagener, T., 2015. A Matlab toolbox for Global Sensitivity  
668 Analysis (Short communication). *Environmental Modelling & Software*, 70, 80-85.  
669 <https://doi.org/10.1016/j.envsoft.2015.04.009>
- 670 Paniconi, C., and Putti, M., 2015. Physically based modeling in catchment hydrology at  
671 50: Survey and outlook Authors. *Water Resources Research*, 51(9), 7090-7129.  
672 <https://doi.org/10.1002/2015WR017780>
- 673 Ponce, V.M., and Simons, D.B., 1977. Shallow wave propagation in open-channel flow,  
674 *Journal of the Hydraulics Division of the American Society of Civil Engineers*,  
675 103(HY 12), 1461-1476.
- 676 Radojkovic, M., and Maksimovic, C., 1987. On standardization of computational models  
677 for overland flow. *Proc., 4th Int. Conf on Urban Storm Drain.*, B. C. Yen, ed.,  
678 International Association for Hydraulic Research, Lausanne, Switzerland, 100-105.
- 679 Ragan, R.M., and Duru, J.O., 1972. Kinematic wave nomograph for times of  
680 concentration. *J. Hydr. Div., ASCE*, 98(10), 1765-1771. [https://doi.org/10.1016/0309-1708\(94\)90009-4](https://doi.org/10.1016/0309-1708(94)90009-4)
- 681
- 682 Rajabi, M., Ataie-Ashtiani, B., and Janssen, H., 2015. Efficiency enhancement of  
683 optimized Latin hypercube sampling strategies: Application to Monte Carlo



- 684 uncertainty analysis and meta-modeling. *Advances in Water Resources*, 76, 127-139.  
685 <https://doi.org/10.1016/j.advwatres.2014.12.008>
- 686 Sabzevari, T., Saghafian, B., Talebi, A., and Ardakanian, R., 2013. Time of concentration  
687 of surface flow in complex hillslopes. *Journal of Hydrology and Hydromechanics*, 61,  
688 2013, 4, 269–277. <https://doi.org/10.2478/johh-2013-0034>
- 689 Saltelli, A., Ratto, M., Andres, T., Campolongo, F., Cariboni, J., Gatelli, D., Saisana, M.,  
690 Tarantola, S., 2008. *Global Sensitivity Analysis, The Primer*. Wiley.
- 691 Savat, J., (1977). The hydraulic of sheet flow on a smooth surface and the effect of  
692 simulated rainfall. *Earth Surface Processes*, 2, 125-140.  
693 <https://doi.org/10.1002/esp.3290020205>
- 694 Singh, V.P., 1988. *Hydrologic systems, Vol. I: Rainfall-runoffmodelling*. Prentice-Hall,  
695 Inc., Englewood Cliffs, N.J.
- 696 Singh, V.P., 1996. *Kinematic Wave Modeling in Water Resources, Surface-Water*  
697 *Hydrology*. Wiley: New York, 1399 pp.
- 698 Singh, V.P., 2001. Kinematic wave modelling in water resources: a historical perspective.  
699 *Hydrol. Process.* 15, 671–706. <https://doi.org/10.1002/hyp.99>
- 700 Singh, V.P., 2002. Is hydrology kinematic? *Hydrol. Process.* 16, 667–716.  
701 <https://doi.org/10.1002/hyp.306>
- 702 U.S. Department of Agriculture, Soil Conservation Service (SCS), 1986. *Urban*  
703 *hydrology for small watersheds*. Tech. Rep. No. 55 (TR-55), Washington, D.C.
- 704 U.S. Department of Agriculture, Soil Conservation Service, 1973. *A method for*  
705 *estimating volume and runoff in small watersheds*, TP-149.
- 706 U.S. Department of Transportation, Federal Highway Administration, 1984. *Drainage of*  
707 *highway pavement*, Hydraulic Engineering Circular No. 12, FHWA-TS-84-202,  
708 March 1984.
- 709 Veal, D.G., 1966. *A computer solution of converging subcritical overland flow*. MS  
710 thesis, Department of Civil Engineering, Cornell University: Ithaca, New York.
- 711 Welle, P.I. and Woodward, D., 1986. *Time of Concentration*. Hydrology Technology  
712 Note No. N4, USDA, Soil Conservation Service, NETC, June 17.
- 713 Wenzel, H.G., 1970. *The effect of raindrop impact and surface roughness on sheet flow*.  
714 WRC Res. Rep. No. 34, Water Resources Centre, University of Illinois, Urbana, Ill.
- 715 Wong, T.S.W., 1994. Kinematic wave celerity and time of concentration. *Hydrological*  
716 *Science and Technology*, 10(1-4), 167 -177.

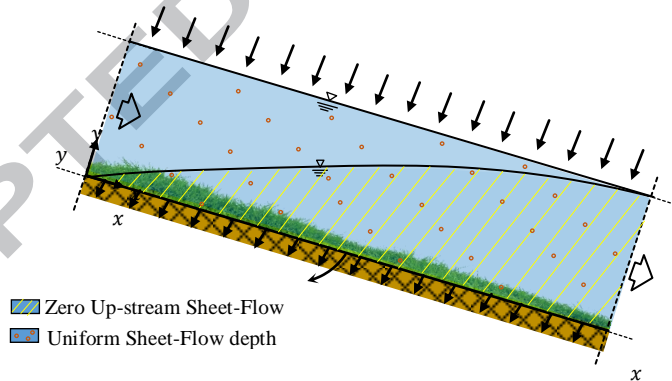
- 717 Wong, T.S.W., 1996. Time of concentration and peak discharge formula for planes in  
718 series. *Journal of Irrigation and Drainage Engineering*, ASCE, 122(4), 256-258.  
719 [https://doi.org/10.1061/\(ASCE\)0733-9437\(1996\)122:4\(256\)](https://doi.org/10.1061/(ASCE)0733-9437(1996)122:4(256))
- 720 Wong, T.S.W., and Chen, Ch.N., 1997. Time of concentration formula for sheet-flow of  
721 varying flow regime, *Journal of Hydrologic Engineering*, 2(3), 136-139.  
722 [https://doi.org/10.1061/\(ASCE\)1084-0699\(1997\)2:3\(136\)](https://doi.org/10.1061/(ASCE)1084-0699(1997)2:3(136))
- 723 Wooding, R.A., 1965. A hydraulic model for the catchment-stream problem. *Journal of*  
724 *Hydrology*, 3, 254-267. [https://doi.org/10.1016/0022-1694\(65\)90084-3](https://doi.org/10.1016/0022-1694(65)90084-3)
- 725 Woolhiser, D.A., Liggett, J.A., 1967. Unsteady one-dimensional flow over a plane: the  
726 rising hydrograph. *Water Resources Research*, 3(3), 753-771.  
727 <https://doi.org/10.1029/WR003i003p00753>
- 728 Yomota, A., and Islam, M.N., 1992. Kinematic analysis of flood runoff for a small-scale  
729 upland field. *Journal of Hydrology*, 137, 311-326. [https://doi.org/10.1016/0022-](https://doi.org/10.1016/0022-1694(92)90062-Z)  
730 [1694\(92\)90062-Z](https://doi.org/10.1016/0022-1694(92)90062-Z)
- 731 Yoon, N.Y., 1970. The effect of rainfall on the mechanics of steady spatially varied sheet  
732 flow, on a hydraulically smooth boundary, Thesis presented to Univ. of Illinois,  
733 Urbana, Ill . , in partial fulfillment of the requirements for the degree of Doctor of  
734 Philosophy.
- 735 Yu, Y.S., and McNown, J.S., 1964. Runoff from impervious surfaces. *Journal of*  
736 *Hydraulic Research*, 2(1), 3-24. <https://doi.org/10.1080/00221686409500069>
- 737
- 738 Zoltani, C.K., 1992. Flow resistance in packed and fluidized beds: an assessment of  
739 current practice. U.S. Army Ballistic Research Laboratory, Technical Report No.  
740 BR1L-TR-3366.



742

Fig. 243. Flowchart of research methodology and process of sheet-flow travel time formulae employed in this study.

744



745

Fig. 246 Unidirectional sheet-flow hydraulics over a planar surface with zero up-stream and uniform flow depth. Rainfall

intensity ( $i$ ), slope ( $S$ ), Manning's roughness coefficient ( $n$ ), and infiltration rate ( $I$ ) are constant over surface.

748

749

750

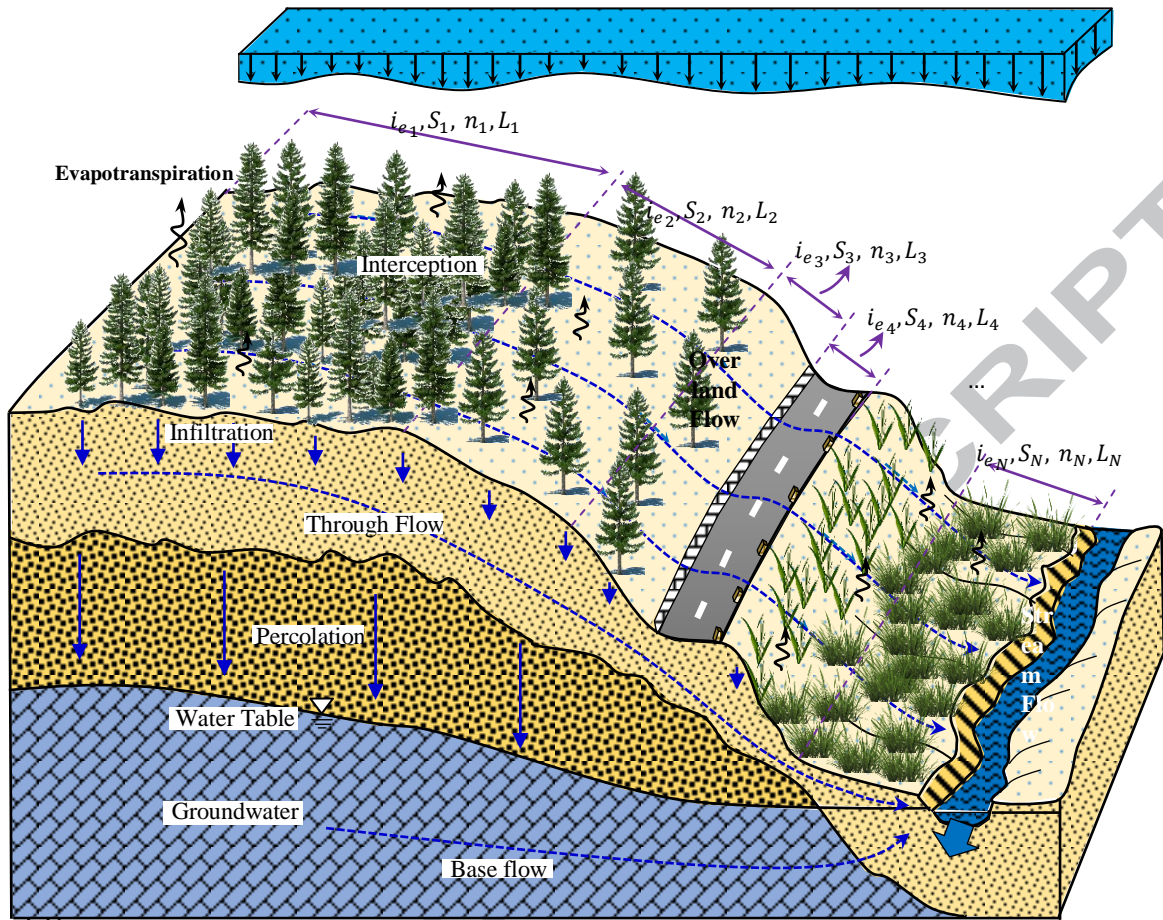
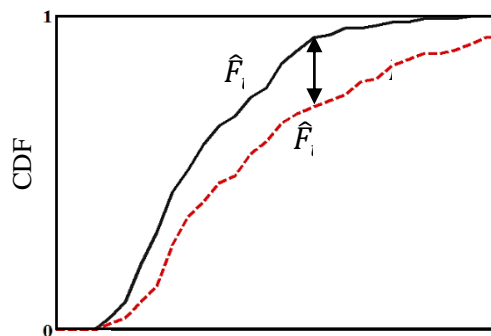


Fig. 752 Schematic of sheet-flow over the cascade of planes with different influential parameters ( $i$  is average rainfall  
 753 intensity,  $i_e$  is average excess rainfall intensity,  $L$  is length of sheet-flow,  $n$  is Manning's roughness coefficient, and  $S$  is  
 754 slope of surface plane).

755

756



757

758 4. Computing the Kolmogorov-Smirnov statistic ( $\hat{KS}$ ) from empirical unconditional and conditional CDFs.

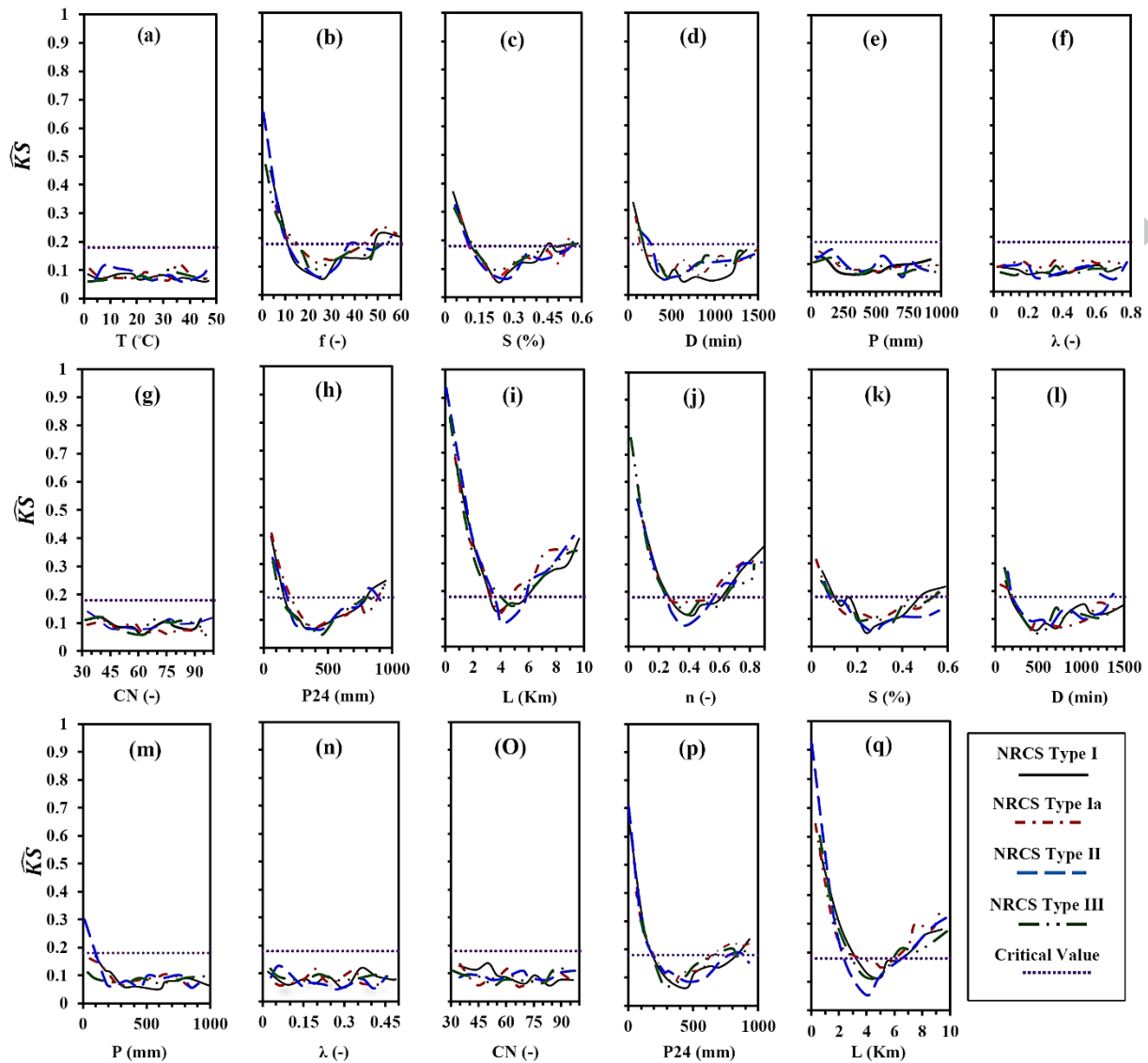


Fig. 760 Kolmogorov–Smirnov statistic ( $\widehat{KS}$ ) at different conditioning values of parameters of the kinematic wave  
 761 model with (a-i) Darcy-Weisbach model (K-D), and (j-q) Manning formula with zero-upstream boundary condition  
 762 (K-M). For all cases,  $\alpha=0.05$ ,  $n' = 10$ ,  $N_u = 100$ , and  $N_c = 50$ .

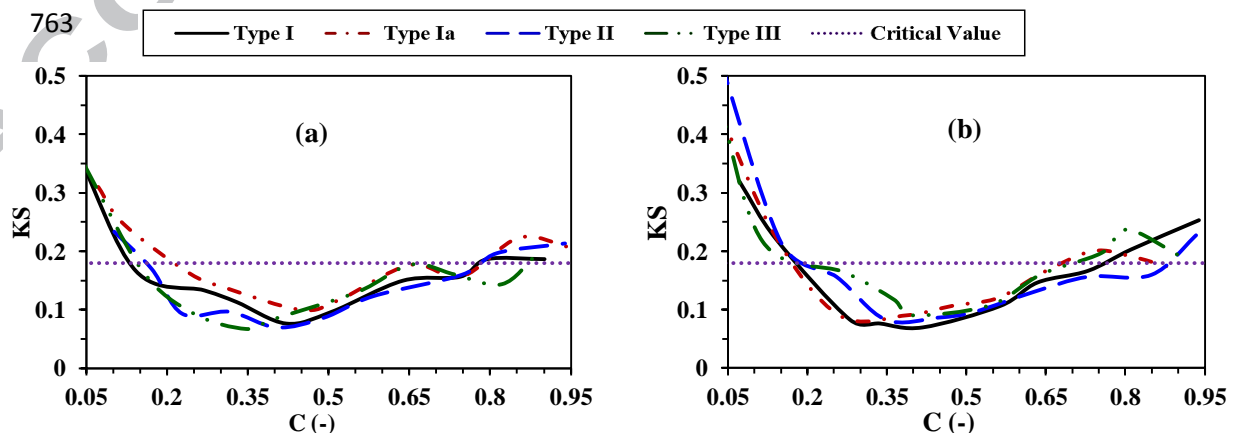


Fig. 764 Sensitivity index ( $\widehat{KS}$ ) of sheet-flow travel time ( $t_{SHF}$ ) to runoff coefficient ( $C$ ) estimated by (a) kinematic  
 765 Darcy-Weisbach formula (K-D) and (b) kinematic Manning formula (K-M) for four types of NRCS design storms.

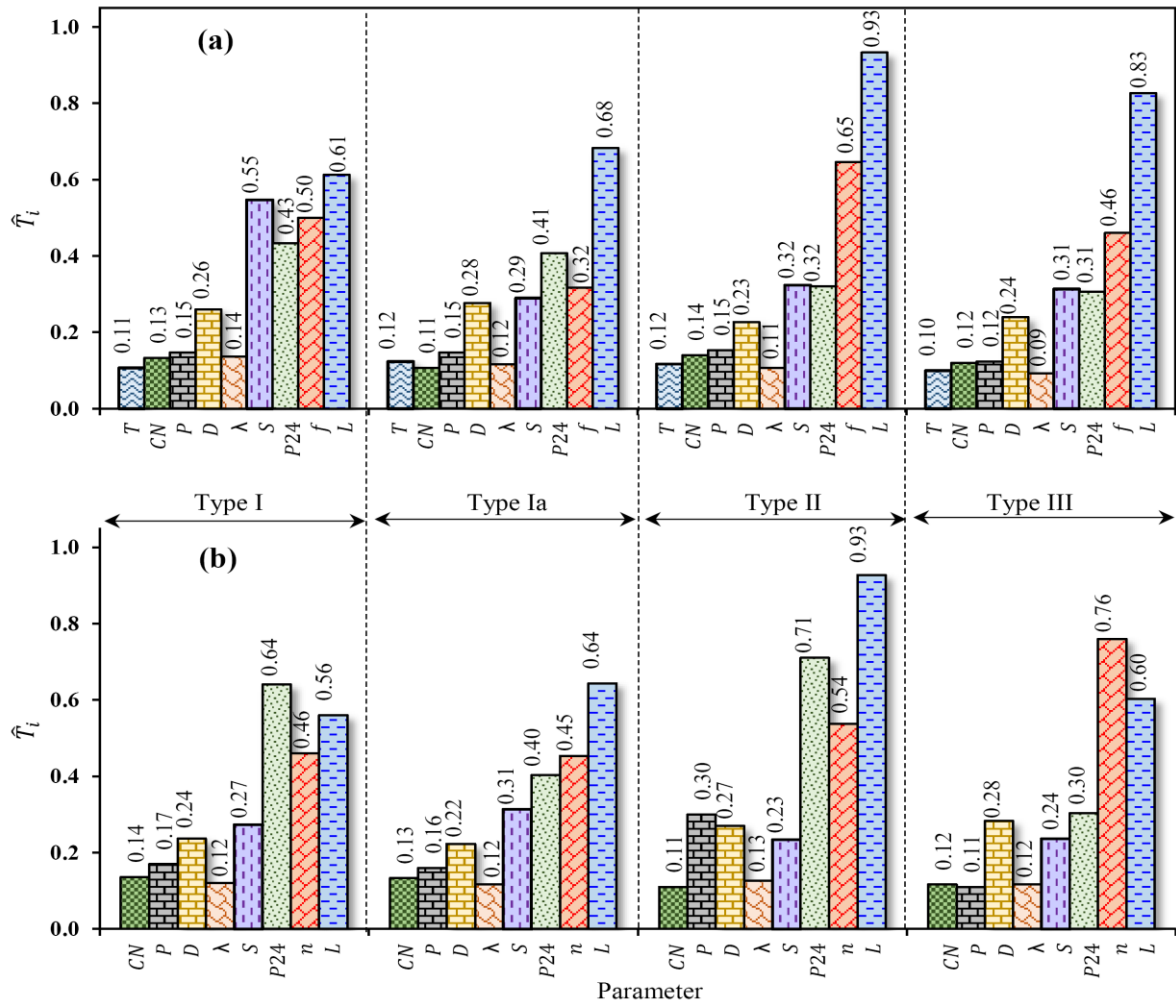
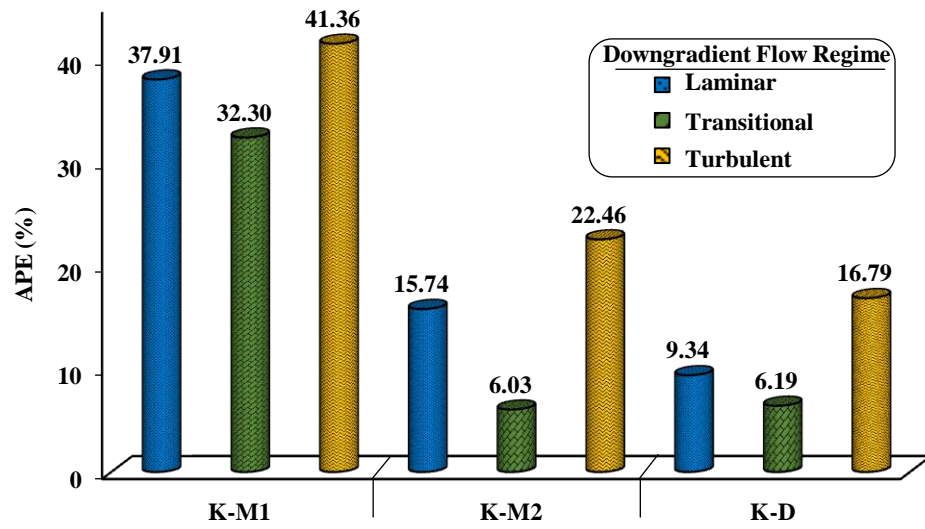


Fig. 768 Sensitivity indices ( $\hat{T}_i$ ) of the sheet-flow travel time to the input parameters estimated by kinematic wave model compared by (a) Manning formula with zero-upstream boundary condition (K-M2), and (b) Darcy-Weisbach formula (K-D)

771

772

773



774

Fig. 875 The average percentage of errors (APE) of K-M1, K-M2, and K-D formulae for estimation of sheet-flow travel  
 time 776 for a single plane surface computed for different downgradient flow regimes (see also data in Table 3).

777

778

779

780

781

782

783

784

785

786

787

788 **Table 1.** Definition of terms and five approximations of Saint-Venant equations (Henderson, 1966).

No.	Term in Saint-Venant eq. (Motion/Continuity)	Formulation of term*	Solution model	Terms of St-Venant included in the solution model
I	Local Inertia (Motion)	$\frac{1}{g} \frac{\partial V}{\partial t} = 0$	Kinematic Wave	IV, V
II	Convective Inertia (Motion)	$\frac{V}{g} \frac{\partial V}{\partial x} = 0$	Diffusion Wave	III, IV, V
III	Pressure Differential (Motion)	$\frac{\partial y}{\partial x} = 0$	Steady Dynamic Wave	II, III, IV, V
IV	Bed and Friction Slope (Motion)	$S_f - S = 0$	Gravity	I, II, III, V
V	Continuity	$\frac{\partial y}{\partial t} + \frac{\partial q}{\partial x} = i_e$	Dynamic Wave	I, II, III, IV, V

\*  $V [L T^{-1}]$  is flow velocity,  $x [L]$  is distance in flow direction,  $g [L T^{-2}]$  is acceleration due to gravity,  $t [T]$  is time,  $y [L]$  is depth of flow,  $S_f [L L^{-1}]$  is friction slope,  $S [L L^{-1}]$  is surface slope (or bed slope),  $q [L^2 T^{-1}]$  is unit discharge of flow.

789

790

791

792

793

794

795

796

797

798

799

800

801

802

803

804

805

806

807

808

809

810

811

812

813



**Table 2.** Observed and estimated sheet-flow travel time ( $t_{SHF}$ ) by kinematic wave theory in combination with Manning formulas considering zero-upstream boundary condition,  $q_u = q_d$  (K-M1) and uniform flow condition,  $q_u = 0$  (K-M2), and kinematic wave in combination with Darcy-Weisbach formula (K-D) in the case of a single plane surface\*.

No.	Surface	Experimental Data						Observed $T_{SHF}$ (s)	Calculated $T_{SHF}$ (s)			Downgradient Flow Regime	Reference of Experimental Data
		$L$ (m)	$S$ (%)	$n$ (-)	(-)	$i_e$ (mm/hr)	Other Parameters		K-M2	K-M1	K-D		
1	Crop		28.4	0.136	6.55	<u>390.0</u> ***	$y_d=4.70$ mm $V=0.092$ m/s	43.48	47.32	26.66	46.35		
2	Crop		27.2	0.103	6.67	<u>440.0</u>	$y_d=4.40$ mm $V=0.011$ m/s	36.03	31.90	22.80	41.70		
3	Fallow	4.0	24.7	0.09	5.02	<u>190.0</u>	$y_d=2.35$ mm $V=0.09$ m/s	44.44	42.30	30.22	41.68	Transitional	Hessel et al. (2003)
4	Orchard		45.8	0.10	7.29	<u>350.0</u>	$y_d=3.0$ mm $V=0.13$ m/s	30.76	29.31	20.94	28.90		
5	Wood		42.6	0.17	23.28	<u>110.0</u>	$y_d=2.02$ mm $V=0.06$ m/s	66.67	65.77	47.0	65.73		
6	Acrylic Glass	2.0	5.0	0.016	NR**	0.0417	$W=1.0$ m	510	456.6	333.0	540.0	Laminar	Sabzevari et al. (2013)
7	Bare Clay		0.43	0.033	NR	47.5	$q=0.08$ m <sup>2</sup> /s	42.0	44.5	31.8	45.65		
8	Bare Clay	9.15	0.42		NR	37.5	$q=0.20$ m <sup>2</sup> /s	69.7	61.96	44.3	72.90	Laminar	Cahill and Li (2003)
9	Asphalt		0.35	0.013	NR		$q=0.25$ m <sup>2</sup> /s	60.0	37.62	26.87	49.84		
10	Pasture		0.48	0.12	NR	33	$q=0.15$ m <sup>2</sup> /s	240.0	206.74	146.7	214.6		
11	Sand and Bitumen	22.86	1.0	0.059	NR	60.0	$q=0.00038$ m <sup>2</sup> /s	370.0	388.47	277.65	361.3	Transitional	Langford and Turner (1973)
12			0.5			210	$q=0.00098$ m <sup>2</sup> /s	140.0	90.82	64.80	116.74		
13	Aluminum	12.2	1.0	0.016	NR	300	$q=0.00072$ m <sup>2</sup> /s	135.0	63.54	45.32	74.45	Turbulent	Ben-zvi (1984)
14			1.5			225	$q=0.00075$ m <sup>2</sup> /s	108.0	63.54	45.40	81.78		
15			2.0			225	$q=0.00089$ m <sup>2</sup> /s	81.0	59.30	41.63	70.50		
16	Turf	142.3	0.5	0.054	NR	55	$V=0.28$ m/s	1320	1465	1046	1429		
17		142.3	2.0	0.014	NR	190	$y_d=11.5$ mm	240	262.0	187.1	227.4		
18		152.4	2.0			200	$V=0.41$ m/s	270	256.6	183.3	232.8	Turbulent	Yu and McNown (1964)
19	Concrete	101.5	0.5	0.014	NR	60	$y_d=6.0$ mm	610	630.5	450.4	591.2		
20		152.4	0.5			20	$V=0.28$ m/s	1200	976.9	697.8	964.3		
21						55	$V=0.20$ m/s	900	706.2	504.4	727.6		

\*  $L$  is length of surface plane,  $W$  is width of surface plane,  $S$  is slope of surface plane,  $n$  is Manning's roughness coefficient of surface,  $f$  is Darcy-Weisbach roughness coefficient,  $i_e$  is effective rainfall intensity,  $y_d$  is downgradient flow depth,  $V$  is downgradient flow velocity, and  $q$  is unit discharge at downgradient of surface plane.

\*\* NR= Not reported in the corresponding reference.

\*\*\* Underlined values are computed from the other parameters.



G→T	3.				0.																
→C	0				2	91.4	133.8	29	42	12	19	0.	75.	73	99.	48	26	81.	11	39	32
	1.				0.			.2	.3	1.6	6.7	2	.3	5	.9	.2	7	4.4	.2	.6	
	0				5																
	0.				9																
	5																				

814

815

816

817

**Highlights:**

819 Physically based estimation of sheet-flow travel time are reviewed.

820 Global sensitivity analysis of the  $t_{SHF}$  formulations are carried out.

821 NRCS design storms are used to consider the variation of rainfall intensity.

822 Darcy-Weisbach is more proficient than the Manning in estimation of the  $t_{SHF}$ .

823

824

825

826

827

828

829

830

831

832

833

834

835

836

837

838